Termination of Cardiac Ca^{2+} Sparks: An Investigative Mathematical Model of Calcium-Induced Calcium Release

Eric A. Sobie,* Keith W. Dilly,* Jader dos Santos Cruz,* W. Jonathan Lederer,* and M. Saleet Jafri†
*Medical Biotechnology Center, University of Maryland Biotechnology Center, Baltimore, Maryland 21201, and †Department of Mathematical Sciences, The University of Texas at Dallas, Richardson, Texas 75083 USA

ABSTRACT A Ca^{2+} spark arises when a cluster of sarcoplasmic reticulum (SR) channels (ryanodine receptors or RyRs) opens to release calcium in a locally regenerative manner. Normally triggered by Ca^{2+} influx across the sarcolemmal or transverse tubule membrane neighboring the cluster, the Ca^{2+} spark has been shown to be the elementary Ca^{2+} signaling event of excitation–contraction coupling in heart muscle. However, the question of how the Ca^{2+} spark terminates remains a central, unresolved issue. Here we present a new model, "sticky cluster," of SR Ca^{2+} release that simulates Ca^{2+} spark behavior and enables robust Ca^{2+} spark termination. Two newly documented features of RyR behavior have been incorporated in this otherwise simple model: "coupled gating" and an opening rate that depends on SR lumenal $[Ca^{2+}]$. Using a Monte Carlo method, local Ca^{2+}-induced Ca^{2+} release from clusters containing between 10 and 100 RyRs is modeled. After release is triggered, Ca^{2+} flux from RyRs diffuses into the cytosol and binds to intracellular buffers and the fluorescent Ca^{2+} indicator fluo-3 to produce the model Ca^{2+} spark. Ca^{2+} sparks generated by the sticky cluster model resemble those observed experimentally, and Ca^{2+} spark duration and amplitude are largely insensitive to the number of RyRs in a cluster. As expected from heart cell investigation, the spontaneous Ca^{2+} spark rate in the model increases with elevated cytosolic or SR lumenal $[Ca^{2+}]$. Furthermore, reduction of RyR coupling leads to prolonged model Ca^{2+} sparks just as treatment with FK506 lengthens Ca^{2+} sparks in heart cells. This new model of Ca^{2+} spark behavior provides a "proof of principle" test of a new hypothesis for Ca^{2+} spark termination and reproduces critical features of Ca^{2+} sparks observed experimentally.

INTRODUCTION

A critical step in cardiac excitation–contraction coupling is the activation of Ca^{2+} sparks (Cheng et al., 1993; Cannell et al., 1994) by voltage-gated Ca^{2+} influx through sarcolemmal L-type Ca^{2+} channels (Cannell et al., 1994, 1995) located in the sarcolemmal (SL) and transverse tubule (TT) membranes (Cheng et al., 1994, 1996a; Shacklock et al., 1995) (see Fig. 1). When an L-type channel opens, intracellular calcium ($[Ca^{2+}]_i$) is elevated close to the channel, in the region between the sarcolemmal and sarcoplasmic reticulum (SR) membranes (also called the "fuzzy space" or the "subspace" (Lederer et al., 1990; Soeller and Cannell, 1997; Jafri et al., 1998)). This local elevation of $[Ca^{2+}]_i$ triggers SR Ca^{2+}-release channels (i.e., ryanodine receptors or RyRs), located in the same subspace, to open and release a greater amount of Ca^{2+} from the SR. This Ca^{2+} released from the SR via RyRs underlies the large, local increase in $[Ca^{2+}]_i$ that is visualized as a Ca^{2+} spark. The process that activates Ca^{2+} sparks therefore displays both high gain (a small amount of "trigger Ca^{2+}" activates a large amount of released Ca^{2+}) and positive feedback (release of Ca^{2+} raises $[Ca^{2+}]_i$ and tends to trigger more release). These characteristics can, in principle, defeat controlled Ca^{2+} release from the SR (Stern, 1992). The fact that Ca^{2+} release is controlled locally (Niggli and Lederer, 1990) helps to overcome potential instabilities (Stern, 1992). However, the picture is currently incomplete because of the uncertainty surrounding the mechanisms that account for the termination of Ca^{2+} sparks.

To date, three distinctive explanations for Ca^{2+} spark termination have been put forward, but each hypothesis has specific weaknesses.

1. The SR could simply run out of releasable Ca^{2+}. Such SR exhaustion models, however, are contradicted at the global level by evidence of substantial SR Ca^{2+} reserves (nonzero SR Ca^{2+} content) following Ca^{2+} release (Varro et al., 1993; Bassani et al., 1995; Negretti et al., 1995), and, at the local level, by the existence of prolonged (lasting seconds) Ca^{2+} sparks (Cheng et al., 1993).
2. The SR Ca^{2+} release process could undergo Ca^{2+}-dependent or use-dependent inactivation or adaptation (Fabiato, 1985; Lukyanenko et al., 1998; Sham et al., 1998). However, examination of gating of RyRs shows that these processes occur too slowly (Györke and Fill, 1993; Valdivia et al., 1995; Fill et al., 2000b) or inadequately (Näbauer and Morad, 1990) to account for termination of the Ca^{2+} transient or the Ca^{2+} spark.
3. All the RyRs in a cluster could by chance close at the same time (termed "stochastic attrition") (Stern, 1992). This mechanism is always present to some extent (Stern et al., 1999) and can work in concert with other mechanisms, but stochastic attrition fails to provide a robust control mechanism when more than a few RyRs are present in a cluster (Stern, 1992) (also see below). The

Submitted August 6, 2001 and accepted for publication March 11, 2002.

Drs. Sobie and Jafri are equal contributors to this paper.

Address reprint requests to W. J. Lederer, Medical Biotechnology Center, UMBI, 725 W. Lombard Street, Baltimore, MD 21201. Tel: 410-706-4895; Fax: 253-660-4449; E-mail: lederer@umbi.umd.edu.

0006-3495/02/07/59/20 $2.00

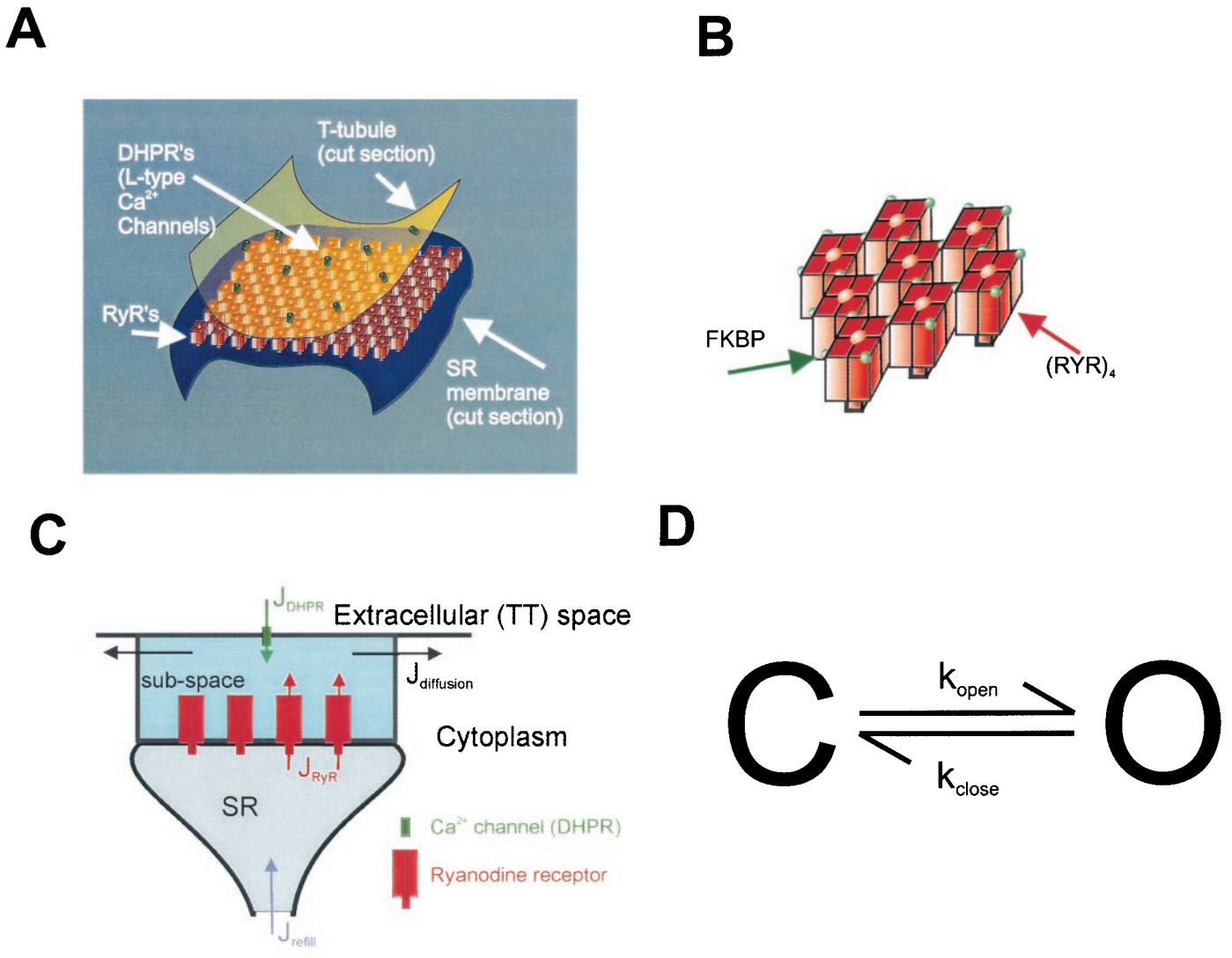

FIGURE 1 Structural considerations and model schematic. (*A*) View of SR–TT junction showing cut section of TT membrane (*transparent yellow*) containing L-type Ca^{2+} channels (DHPR) (*green*). The TT containing DHPRs is closely apposed to an SR release unit composed of 100 RyRs (*red*). (*B*) Close-up view of 8 RyRs taken from (*A*). The green spheres represent FKBP12.6 proteins that mediate interactions between neighboring RyR homotetramers and are found close to points of contact. (*C*) Layout of the model elements. Ca^{2+} passing through a single L-type channel enters the subspace between the TT and SR membranes and can trigger release from a cluster of RyRs located in the junctional SR. In addition to channel fluxes of Ca^{2+}, diffusion of Ca^{2+} from the subspace to the cytoplasm (J_{efflux}) and refilling of the junction from neighboring SR (J_{refill}) determine Ca^{2+} concentrations in the subspace ($[Ca^{2+}]_{SS}$) and the local JSR lumen ($[Ca^{2+}]_{lumen}$). (*D*) RyR gating. Each RyR homotetramer is modeled with only a single open and a single closed state, without any adaptation or inactivation processes. Opening and closing rates depend on $[Ca^{2+}]_{SS}$, $[Ca^{2+}]_{lumen}$, and coupled gating of RyRs, as described in Methods.

absence of a viable model of Ca^{2+} spark termination is one of the biggest defects in our current concept of excitation–contraction coupling, as recent reviews have stressed (Niggli, 1999; Wier and Balke, 1999; Cannell and Soeller, 1999).

Three new results regarding the anatomy of the junctions between the SR and the TT in heart have considerable bearing on our understanding of Ca^{2+} sparks. First, the SR–TT junction contains nearly crystalline arrays of RyRs organized in clusters (Franzini-Armstrong et al., 1998, 1999). The number of RyRs in a cluster depends on species, but averages ~100. Second, the RyRs are organized as homotetrameric units, each touching four neighbors with a small protein, FK-binding protein (FKBP) at or near the point of contact (See Fig. 1, *A* and *B*) (Wagenknecht et al., 1997; Samso and Wagenknecht, 1998; Sharma et al., 1998). Third, RyRs incorporated into planar lipid bilayers can exhibit coupled gating, whereby two or more channels display synchronized openings and closings (Marx et al., 1998, 2001). These findings suggested to us that the clustering of

the RyRs and the physical contact between homotetrameric RyRs may be functionally important.

An additional recent result is also important to our understanding of the regulation of cardiac calcium-induced calcium release (CICR). As suggested by experiments in heart cells (Cheng et al., 1996b; Lukyanenko et al., 1996), studies in planar lipid bilayers (Thedford et al., 1994; Gyorke and Gyorke, 1998; Ching et al., 2000) and cardiac vesicles (Ikemoto et al., 1989) have confirmed that Ca^{2+} in the SR lumen can influence RyR gating such that RyRs are more likely to be triggered by cytosolic Ca^{2+} when SR lumenal Ca^{2+} is elevated.

In the present study, we incorporate these new results into a mathematical model of cardiac Ca^{2+} sparks and put forward a new hypothesis, sticky cluster, to describe the behavior of Ca^{2+} sparks in heart. This hypothesis addresses two fundamental holes in our understanding of Ca^{2+} sparks, namely, how termination of Ca^{2+} sparks occurs, and what influence the large but variable number of RyRs in a cluster may have upon Ca^{2+} spark behavior. In the sticky cluster model, Ca^{2+} spark termination results from two factors: the influence of lumenal [Ca^{2+}] on RyR gating, and coupled gating between the RyRs in a cluster. Furthermore, this model produces Ca^{2+} sparks that terminate robustly in a manner that is largely independent of the number of RyRs in a cluster. Additionally, the model simulates the occurrence of spontaneous sparks at a realistic rate, and is consistent broadly with experimental results, including those that reveal that Ca^{2+} sparks can be prolonged under certain conditions.

METHODS

Cell isolation and confocal imaging

Adult mice were killed by intraperitoneal injection of pentobarbital (100 mg/kg), and single ventricular myocytes were isolated (Cannell et al., 1995) and stored at room temperature (22–25°C) in Dulbecco's modified Eagle's medium (JRH Biosciences, Lanexa, KS) until used. Cells were loaded with fluo-3 by exposure to 5.5 μM fluo-3AM for 30 min at room temperature. Cells were superfused with NaCl 140 mM, KCl 5 mM, $MgCl_2$ 0.5 mM, $CaCl_2$ 1.8 mM, NaH_2PO_4 0.33 mM, Glucose 5.5 mM, HEPES 5 mM. The pH of all extracellular solutions was kept at 7.4 with the temperature at 34–37°C. Confocal microscopy was used to measure Ca^{2+} sparks as described previously (Cheng et al., 1993; Cannell et al., 1994, 1995).

Model Layout

The model is separated into two independent components: 1) Mathematical description of SR Ca^{2+} release through an RyR cluster at the SR–TT junction. This component of the model contains the major novel features of our presentation. 2) Mathematical description of the Ca^{2+} spark produced by the Ca^{2+} efflux. This component of the model refines earlier descriptions of the diffusion, buffering, and imaging processes that produce the Ca^{2+} spark (Smith et al., 1998). Figure 1 *C*, which illustrates the model schematically, shows that it consists of a single L-type Ca^{2+} channel (also called a dihydropyridine receptor, DHPR) closely apposed to a cluster of RyRs in a region of junctional sarcoplasmic reticulum (JSR). The channels communicate through changes in [Ca^{2+}] in a restricted subsarcolemmal space (subspace, SS). The following Ca^{2+} fluxes determine Ca^{2+} concentrations in the subspace and the local, JSR lumen ($[Ca^{2+}]_{lumen}$): fluxes through the L-type channel (J_{DHPR}) and the RyRs ($J_{release}$), binding of Ca^{2+} to buffers in the subspace (J_{buf}), efflux from the subspace to the bulk myoplasm via diffusion (J_{efflux}), and refilling of the SR lumen by diffusion from neighboring network SR (J_{refill}). Thus, $[Ca^{2+}]_{SS}$ is described by the balance equation,

TABLE 1 Geometry parameters

Parameter	Definition	Value
V_{SS}	Subspace volume	1.0×10^{-13} μL
V_{JSR}	JSR volume	1.0×10^{-11} μL
τ_{efflux}	SS efflux time constant	7.0×10^{-7} s
τ_{refill}	JSR refilling time constant	0.01 s
$[Ca^{2+}]_{myo}$	Bulk myoplasmic Ca^{2+} concentration	0.1 μM
$[Ca^{2+}]_{NSR}$	NSR Ca^{2+} concentration	1.0 mM

$$\frac{d[Ca^{2+}]_{SS}}{dt} = J_{release} + J_{DHPR} + J_{efflux} + J_{buf}. \quad (1)$$

A description of how the individual fluxes are calculated follows.

Fluxes through the Ca^{2+} channels (DHPR and RyRs) depend on channel permeability, the concentration gradient for Ca^{2+}, and whether the channels are open. Thus, $J_{DHPR} = 0$ when the channel is closed, and

$$J_{DHPR} = -\frac{\bar{I}_{DHPR}}{2FV_{SS}} \quad (2)$$

when the channel is open, where $\bar{I}_{DHPR}$ is the single-channel L-type current, F is Faraday's constant, and V_{SS} is the subspace volume (values given in Table 1). Similarly, flux through a single, open RyR is calculated as

$$J_{RyR} = D_{RyR}([Ca^{2+}]_{lumen} - [Ca^{2+}]_{SS}) \quad (3)$$

where D_{RyR} reflects the ease with which Ca^{2+} passes through an open RyR. The total Ca^{2+} release flux, $J_{release}$, simply reflects the flux through all the open RyRs in the cluster, i.e.,

$$J_{release} = \sum_{i=1}^{N} RyR^{i}_{open} J_{RyR} \quad (4)$$

where $RyR^{i}_{open} = 0$ if channel i is closed, 1 if it is open, and N represents the number of channels in the cluster. We set $N = 50$ in control conditions. However, given the variability in cluster size observed experimentally, it is important to verify that Ca^{2+} sparks produced by clusters of various sizes can terminate robustly.

Ca^{2+} in the subspace can be bound to SL and SR membrane buffers and calmodulin (CaM), with buffer characteristics based on those reported previously (Smith et al., 1998). Thus,

$$J_{buf} = \sum_{i=CaM,SR,SL} k^{i}_{on}[Ca^{2+}]_{SS}[B_i] - k^{i}_{off}([B_i]_{tot} - [B_i]), \quad (5)$$

where k^{i}_{on} is the Ca^{2+} on rate, k^{i}_{off} the Ca^{2+} off rate, $[B_i]$ is the unbound buffer concentration, and $[B_i]_{tot}$ is the total concentration (bound + unbound) of buffer i.

Efflux of Ca^{2+} from the subspace via diffusion to the myoplasm is calculated as

$$J_{efflux} = \frac{[Ca^{2+}]_{myo} - [Ca^{2+}]_{SS}}{\tau_{efflux}}, \quad (6)$$

with $[Ca^{2+}]_{myo}$ held fixed at 0.1 μM, and τ_{efflux} is the time constant for Ca^{2+} transfer between the subspace and the bulk myoplasm. The different time constants for transfer to the bulk cytoplasm (τ_{efflux}) and within the SR (τ_{refill}) reflect the assumption that these two diffusion processes will typically occur over different characteristic distances. These time constants are roughly equivalent to diffusion over a spatial scale of, respectively, 8–13 nm and 0.5–1.58 μm (depending on whether the true or an effective diffusion constant for Ca^{2+} is assumed). This flux of Ca^{2+} from the subspace to the myoplasm is used as the input for the second model (described below) that simulates the production of Ca^{2+} sparks.

The balance equation for JSR lumenal Ca^{2+} concentration ($[Ca^{2+}]_{lumen}$) is

$$\frac{d[Ca^{2+}]_{lumen}}{dt} = \beta_{JSR}\left(- J_{RyR}\frac{V_{SS}}{V_{JSR}} + J_{refill}\right), \quad (7)$$

where the JSR is depleted by RyR Ca^{2+} release scaled by the ratio of subspace volume (V_{SS}) to JSR volume (V_{JSR}) and refilled from the network sarcoplasmic reticulum (NSR) by J_{refill},

$$J_{refill} = \frac{[Ca^{2+}]_{NSR} - [Ca^{2+}]_{lumen}}{\tau_{refill}}, \quad (8)$$

with $[Ca^{2+}]_{NSR}$ held fixed at 1.0 mM and τ_{refill} is the time constant for Ca^{2+} transfer between the JSR and NSR. Buffering in the JSR by calsequestrin uses the rapid buffering approximation (Keizer and Levine, 1996) given by

$$\beta_{JSR} = \left[1 + \frac{[CSQ]_{tot}K_{CSQ}}{(K_{CSQ} + [CSQ])^2}\right]^{-1}, \quad (9)$$

where $[CSQ]_{tot}$, $[CSQ]$, and K_{CSQ} represent the total concentration, unbound concentration, and Ca^{2+}-dissociation constant, respectively, of calsequestrin.

Ryanodine receptor gating

The primary goal of the present study is to gain insight into Ca^{2+} spark behavior and the mechanisms of spark termination by investigating how the features of RyR gating in the sticky cluster influence Ca^{2+} spark characteristics. Because, in cardiac muscle, Ca^{2+} spark termination occurs independently of spark triggering (Cheng et al., 1993; Cannell et al., 1995), we did not simulate the gating of the DHPR. In most simulations, we initiated a Ca^{2+} spark with a stereotypical DHPR opening (0.5 pA, 0.5 ms) that could trigger a spark with >98% fidelity. The details of the gating of an RyR in a cluster follow.

The 50 RyRs are assumed to gate independently except for a "coupling" or "cooperativity" factor (CF_{close} and CF_{open} as defined below). Each RyR is modeled with only a single closed and a single open state and no adaptation or other inactivation processes over the time scale of the Ca^{2+} spark (Fig. 1 *D*). We exclude these features for the sake of simplicity and to demonstrate that they are not necessary for spark termination. We do not mean to argue against a role for these phenomena in regulating cardiac Ca^{2+} signaling. Thus, in this model, any intervention that alters the gating behavior of the RyR cluster must do so by modifying either the opening rate, k_{open}, or the closing rate, k_{close}.

The RyR closing rate was independent of $[Ca^{2+}]_{SS}$,

$$k_{close} = CF_{close} \times 480.0\ s^{-1}, \quad (10)$$

whereas the opening rate was a fourth-order function of $[Ca^{2+}]_{SS}$,

$$k_{open} = 3.0 \times 10^4 \cdot CF_{open}\frac{[Ca]_{ss}^4}{[Ca]_{ss}^4 + K_m^4}\ s^{-1}. \quad (11)$$

Lumenal Ca^{2+} influences RyR gating through changes in K_m in the above equation. Sensitivity to $[Ca^{2+}]_{SS}$ is a linear, decreasing function of $[Ca^{2+}]_{lumen}$, so that RyR opening is favored when $[Ca^{2+}]_{lumen}$ is high, as suggested by the literature (Thedford et al., 1994; Cheng et al., 1996b; Gyorke and Gyorke, 1998; Lukyanenko et al., 1998; Ching et al., 2000):

$$K_m = 6.0 - 0.0024[Ca^{2+}]_{lumen}\ \mu M. \quad (12)$$

Coupled gating of RyRs is introduced by multiplying the opening and closing rate constants by cooperativity factors (CF_{open} for opening and CF_{closed} for closing) that depend, respectively, on the relative numbers of open and closed channels in the cluster,

$$CF_{open} = 1 + \frac{N_{open} + 1}{N_{open} + N_{closed}}, \quad (13)$$

$$CF_{close} = k_{coop}\left[1 + \frac{N_{closed} + 1}{N_{open} + N_{closed}}\right], \quad (14)$$

where N_{open} is the number of open RyRs, and N_{closed} is the number of closed RyRs. CF_{open} and CF_{close} are both cooperative in their behavior because the value of either depends on the fraction of open channels. The scaling factor k_{coop} (equal to unity in control conditions) was introduced so that modification of a single parameter could simulate changes in the strength of coupling between RyRs.

TABLE 2 Channel parameters

Parameter	Definition	Value
F	Faraday's constant	96480 C · mol^{-1}
$\bar{I}_{DHPR}$	DHPR single-channel current	−0.5 pA
D_{RyR}	Ca^{2+} diffusion through open RyR parameter	4000.0 s^{-1}

TABLE 3 Buffering parameters

Parameter	Definition	Value
$[B_{CSQ}]_{tot}$	Total calsequestrin concentration	10.0 mM
K_{CSQ}	Calsequestrin Ca^{2+} dissociation constant	0.8 mM
$[B_{CaM}]_{tot}$	Total calmodulin concentration	24.0 μM
k_{on}^{CaM}	Calmodulin Ca^{2+} on-rate constant	100.0 $\mu M^{-1}s^{-1}$
k_{off}^{CaM}	Calmodulin Ca^{2+} off-rate constant	38.0 s^{-1}
$[B_{SR}]_{tot}$	Total SR membrane buffer concentration	47.0 μM
k_{on}^{SR}	SR membrane buffer Ca^{2+} on-rate constant	115.0 μM^{-1} s^{-1}
k_{off}^{CaM}	SR membrane buffer Ca^{2+} off-rate constant	100.0 s^{-1}
$[B_{SL}]_{tot}$	Total SL membrane buffer concentration	1124.0 μM
k_{on}^{SL}	SL membrane buffer Ca^{2+} on-rate constant	115.0 $\mu M^{-1}s^{-1}$
k_{off}^{SL}	SL membrane buffer Ca^{2+} off-rate constant	1000.0 s^{-1}

A Monte Carlo method (Rice et al., 1999) was used to simulate the openings and closings of the RyRs with the Ca^{2+} balance equation solved at each time step using Euler's method. A time step of 10^{-8} s was used in the simulations. The code was implemented in FORTRAN on an HP Visualize unix workstation.

Spark model

The model described above produces as its output a flux of Ca^{2+} from the SS into the myoplasm. To generate Ca^{2+} signals with similar spatiotemporal characteristics to those that would be measured experimentally, we simulated spark generation and detection, based on a method previously published (Smith et al., 1998). This model calculates Ca^{2+} diffusion in the myoplasm (spherical symmetry is assumed), Ca^{2+} binding to fluo-3 and stationary buffers, and blurring by the confocal microscope. The model implemented here is identical to that presented by Smith et al.(1998) with two exceptions: we assume that SL buffers are confined to within 300 nm of the cluster and the concentration of these buffers decreases linearly with distance from the RyR cluster, and we assume a fluo-3 Ca^{2+}-dissociation constant of 0.5 μM, rather than 1.13 μM. These changes were made so that the time course of the model Ca^{2+} spark more closely resembled that typically recorded experimentally: specifically, the original Smith model produced sparks with an unrealistically large amplitude and an unrealistically slow decay after release termination. A semi-implicit algorithm was used to solve for Ca^{2+} dynamics in space and time, such that diffusion of Ca^{2+} and fluo-3 was treated implicitly with a Crank–Nicholson algorithm, and Ca^{2+} buffering was treated explicitly. The model was implemented in Matlab (The Mathworks, Natick, MA), and a time step of 2 μs was used. Results were visualized with IDL and Origin software, and CorelDraw was used to produce figures.

RESULTS

To explain the behavior of Ca^{2+} sparks in intact cells, given the current knowledge of the anatomy, biochemistry, and biophysics of Ca^{2+} signaling in heart, two questions must be addressed: how do Ca^{2+} sparks terminate, and why are Ca^{2+} sparks so similar in duration?

Basic simulation

Figure 2 displays an example of simulated Ca^{2+} release under control conditions, with 50 RyRs in the sticky cluster and a cooperativity factor (k_{coop}) of 1. In this simulation, as in most of the simulations carried out in this study, a stereotypical DHPR opening (0.5 ms, −0.5 pA) triggers CICR in the RyR cluster. Our Monte-Carlo method simulates stochastic openings and closings of RyRs in the cluster (as seen by the noise or chatter in the records shown), and the temporal evolution of each Ca^{2+} release event is slightly different. The composite open probability (P_o) of the 50 RyRs, the resulting Ca^{2+} efflux from the subspace to the myoplasm, and the local JSR lumenal Ca^{2+} concentration ($[Ca^{2+}]_{lumen}$) are displayed in Fig. 2, *A*, *B*, and *C*, respectively. Ca^{2+} entering the subspace (SS) through the DHPR activates release from the cluster by binding to the RyRs and increasing their P_o to a value close to 1. The opening of RyRs increases $[Ca^{2+}]_{SS}$ further, thereby contributing additional Ca^{2+} to the positive feedback of CICR. The composite P_o of the RyRs remains close to 1 for ~10 ms but declines as $[Ca^{2+}]_{lumen}$ (Fig. 2 *C*) and $[Ca^{2+}]_{SS}$ fall and exhibits larger fractional fluctuations until all RyRs close nearly simultaneously (P_o quickly declines to zero) after ~25 ms. The firm closure of the RyRs arises from the gating cooperativity of the RyRs in the cluster. Re-opening is prevented by hysteresis in the relationship between P_o and $[Ca^{2+}]_{SS}$ that is due to the influence of $[Ca^{2+}]_{lumen}$ on this relationship. The Ca^{2+} efflux (Fig. 2 *B*) during the release process reaches an early peak, declines as the local SR lumen becomes depleted of Ca^{2+}, then decreases to zero when the RyRs in the cluster close.

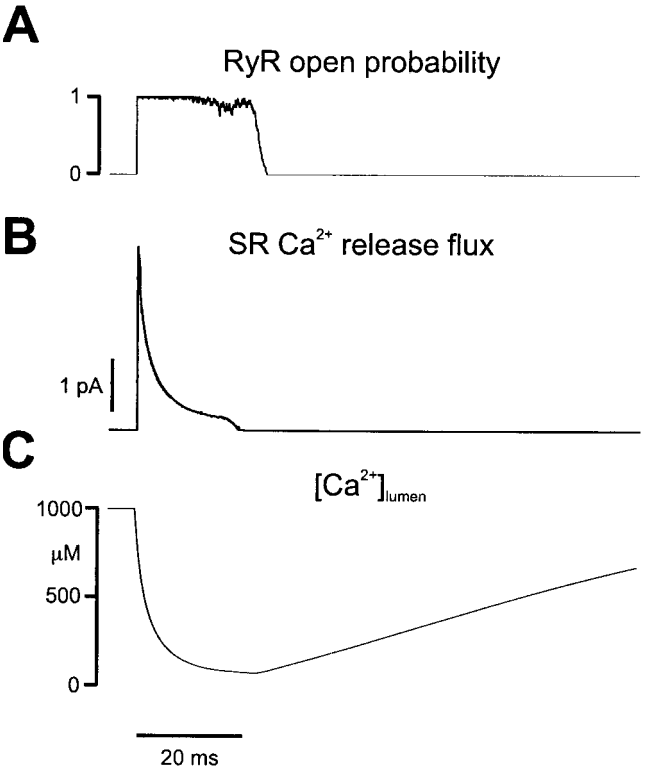

FIGURE 2 Simulated RyR gating and Ca^{2+} fluxes during a typical Ca^{2+} spark. (*A*) Composite open probability (P_o) of the 50 RyRs in the cluster. (*B*) Efflux from the subspace versus time. (*C*) Lumenal Ca^{2+} concentration ($[Ca^{2+}]_{lumen}$) versus time. The decrease in $[Ca^{2+}]_{lumen}$ leads to increased flickering of RyRs and a slight decrease in P_o until the influence of coupled gating causes all RyRs in the cluster to close within 3 ms and not reopen.

The efflux of Ca^{2+} through the cluster of RyRs, when used as an input to the buffering and diffusion model described above, produces a Ca^{2+} spark as shown in Fig. 3. Figure 3 *A* displays a simulated line-scan image of the resulting Ca^{2+} spark, similar to that which would be recorded experimentally (assuming the point of release is located directly on the scan line). The relative level of $[Ca^{2+}]_i$ (measured as F/F_0) is shown in time-profiles of the line-scan image in Fig. 3 *B*, with the color-coded tick marks on the right-hand edge of Fig. 3 *A* indicating that $[Ca^{2+}]_i$ time courses are displayed at the point of release and at

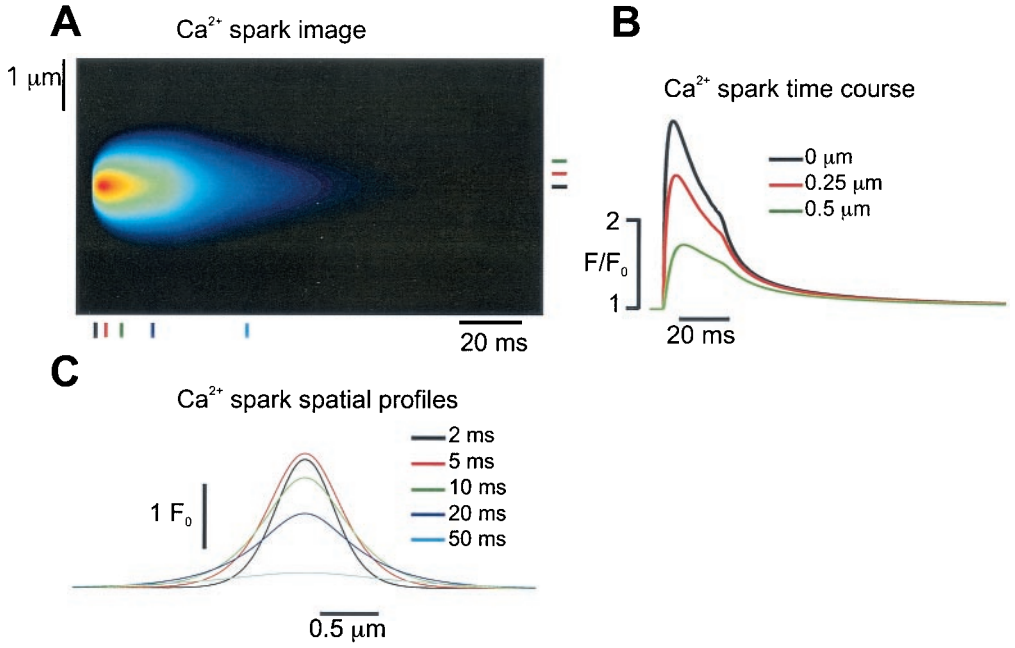

FIGURE 3 Simulated Ca^{2+} spark under control conditions. (*A*) Line scan image of simulated Ca^{2+} spark under control conditions (50 RyRs in cluster, $k_{coop} = 1$). (*B*) Time courses of Ca^{2+} sparks (plotted as F/F_0) at locations 0, 0.25, and 0.5 μm from the source are displayed in black, red, and green, respectively. Locations on line scan are noted to right of the image. (*C*) Ca^{2+} spark spatial profiles 2, 5, 10, 20, and 50 ms after the beginning of the spark are displayed in black, red, green, blue, and, cyan respectively. Times are marked below the image.

distances 0.25 and 0.5 μm from the point of release. The spatial profiles that would be recorded during the Ca^{2+} spark are shown in Fig. 3 *C*. The tick marks on the bottom of Fig. 3 *A* show the times of the profiles, corresponding to 2, 5, 10, 20, and 50 ms after Ca^{2+} spark initiation.

Background noise

Experimentally measured line-scan images of Ca^{2+} sparks exhibit fluctuations in fluorescence intensity due in part to the noise of the system. This noise comes from the excitation laser, the photodetector, amplifiers, and the fluorescent light itself. We characterized the noise recorded in line-scan images of Ca^{2+} sparks and then simulated this noise as normally distributed fluctuations about a mean level. Figure 4 *A* (top) shows the line-scan image of a simulated Ca^{2+} spark with this realistic noise added. The increase in background reflects different scaling of the image after fluctuations around the background are added. The middle and bottom traces, respectively, display the time course of the noisy Ca^{2+} spark at the point of release and averaged over the width of the Ca^{2+} spark. ($\pm$0.5 μm centered on the point of Ca^{2+} release) Figure 4 *B* shows identical records produced by the model with noise added when the cluster comprises only a single RyR. One of the clear effects of the addition of a realistic amount of noise is the loss of the apparent shoulder produced as Ca^{2+} release is terminated. A second observation is that one cannot visually detect the $[Ca^{2+}]_i$ signal resulting from the opening of a single RyR. This is due to the small level of Ca^{2+} release and its short duration. This result, however, provides an explanation for the absence or near invisibility of Ca^{2+} sparks in cell systems with few or extremely small RyR clusters (Bhat et al., 1997; Haak et al., 2001).

Cluster size and RyR flux

In Figs. 2–4, 50 RyRs were arranged in a cluster to simulate a control Ca^{2+} spark; however, because it is likely that the number of RyRs in a cluster may vary widely (Franzini-Armstrong et al., 1998, 1999), we simulated Ca^{2+} sparks produced by clusters of different sizes. Simulations from clusters containing 100, 50, 20, and 10 RyRs are shown in Fig. 5, *A*, *B*, *C*, and *D*, respectively. Each panel displays the SR release flux (*top*), $[Ca^{2+}]_{lumen}$ (*middle*), and the Ca^{2+} spark time course, measured at 0.25 μm from the source (*bottom*). Three features of these simulations are of particular interest. First, SR release terminates robustly at about the same time after it is initiated, leading to Ca^{2+} sparks with similar durations regardless of the number of RyRs in the cluster. Second, termination of Ca^{2+} release occurs at different levels of $[Ca^{2+}]_{lumen}$ as cluster size is varied. This helps to explain the small variation in the duration of release. With fewer RyRs in the cluster, it is more likely that the stochastic closing of a few RyRs will induce the remaining channels to close. However, the decreased peak Ca^{2+}

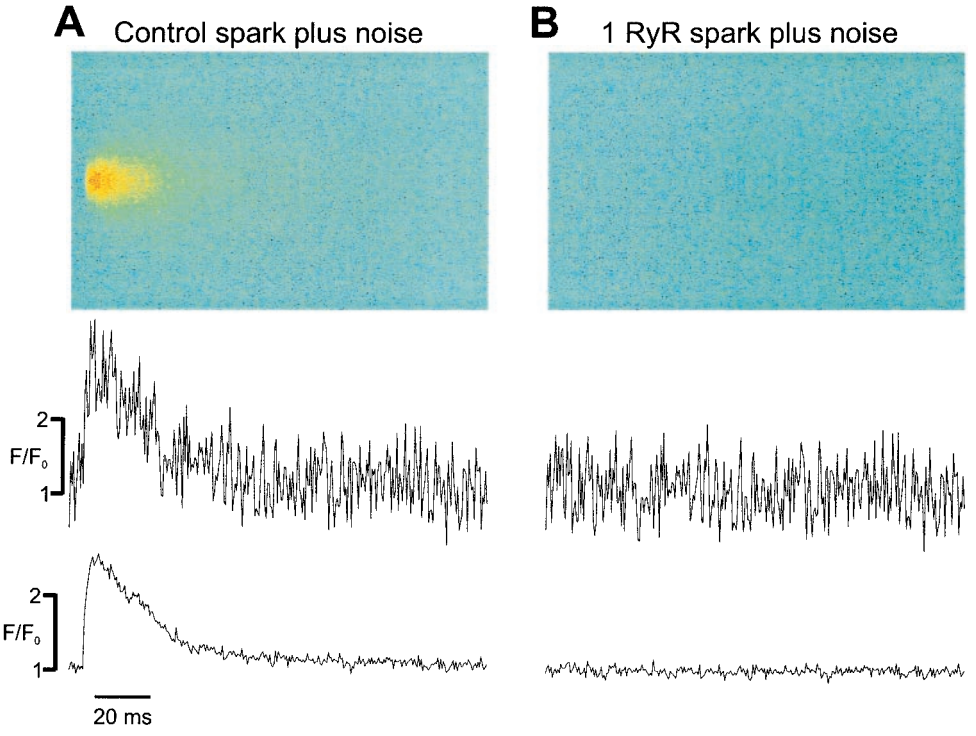

FIGURE 4 Appearance of Ca^{2+} sparks with realistic noise. (*A*) Line-scan image of simulated Ca^{2+} spark that would result from the opening of 50 RyRs with realistic noise added (*top*), time course of $[Ca^{2+}]_i$ as F/F_0 (0.25 μm from source, *middle*) and time course of $[Ca^{2+}]_i$ (averaged over central 1 μm of Ca^{2+} spark, *bottom*). The addition of realistic noise leads to the loss of the inflection in the time course of $[Ca^{2+}]_i$ when release is terminated (see Fig. 3 *B*). See text for details. (*B*) Line-scan image of simulated Ca^{2+} spark with realistic noise that would result from the opening of a single RyR (*top*), time course of $[Ca^{2+}]_i$ as F/F_0 (0.25 μm from source, *middle*) and time course of $[Ca^{2+}]_i$ (averaged over central 1 μm of point of Ca^{2+} release, *bottom*). The fluorescent Ca^{2+} signal is not readily distinguishable from the noise.

efflux leads to slower depletion of $[Ca^{2+}]_{lumen}$. Because P_o depends on $[Ca^{2+}]_{lumen}$, the slower depletion tends to prolong the duration of release. These two effects essentially cancel each other, leading to the relatively constant Ca^{2+} spark duration observed. Third, although the peak of the Ca^{2+} release flux approximately scales with the number of RyRs in a cluster (*top traces*), the peak F/F_0 of a Ca^{2+} spark does not (*bottom traces*). Two explanations appear to ac-

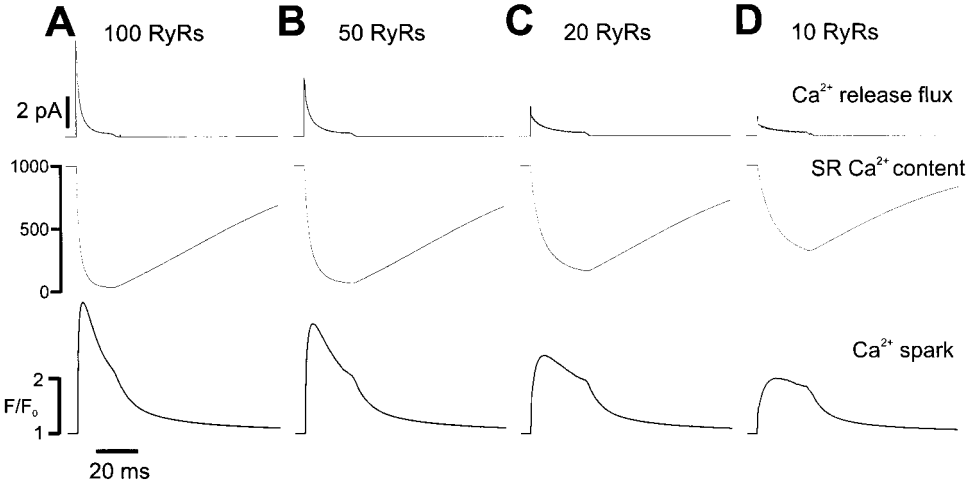

FIGURE 5 Simulated Ca^{2+} sparks resulting from RyR clusters of various sizes. (*A*) 100 RyRs in cluster. Efflux from the subspace (*top*), $[Ca^{2+}]_{lumen}$ (*middle*), and $[Ca^{2+}]_i$ as F/F_0 (measured 0.25 μm from source, *bottom*). (*B*) 50 RyRs in cluster (control conditions). (*C*) 20 RyRs in cluster. (*D*) 10 RyRs in cluster. Varying the number of RyRs in the cluster affects initial efflux significantly, spark amplitude modestly, and spark duration minimally (see Fig. 6).

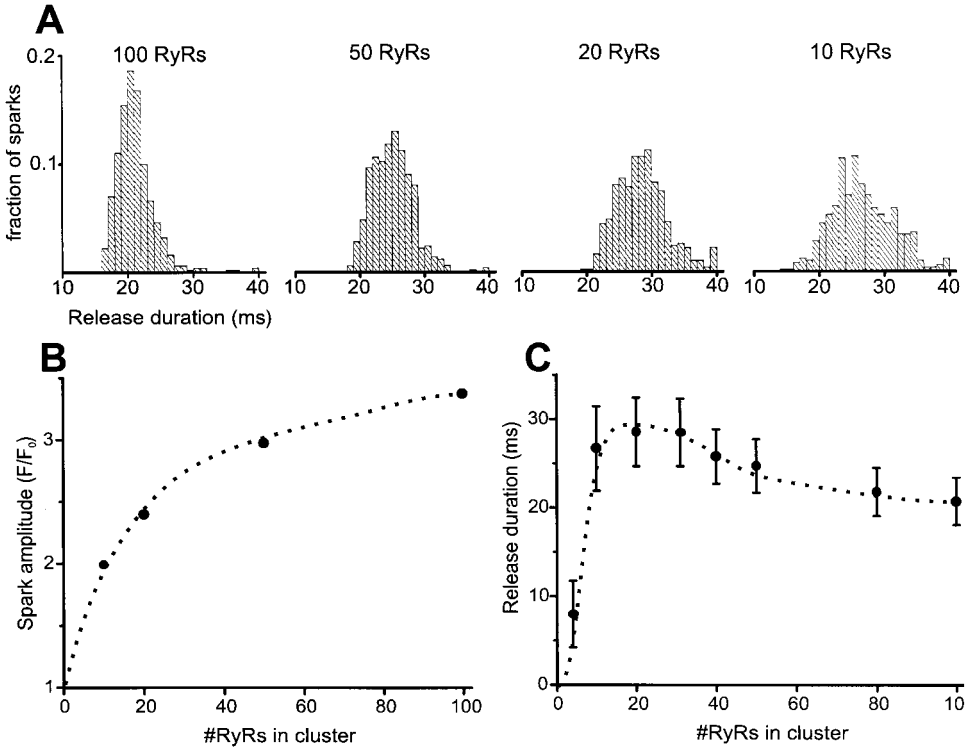

FIGURE 6 Effects of RyR number on Ca^{2+} spark amplitude and duration: population data. (*A*) Histograms of the duration of Ca^{2+} release for 100, 50, 20, and 10 RyRs in cluster. 500 Ca^{2+} sparks were simulated to generate each histogram. (*B*) Peak amplitude of Ca^{2+} sparks (averaged) versus RyR cluster size. An increase in cluster sizes causes a less-than-proportional increase in Ca^{2+} spark amplitude. (*C*) Mean Ca^{2+} spark duration and standard deviation plotted as a function of the number of RyRs in a cluster. Ca^{2+} spark duration reveals a biphasic dependence on number of RyRs in a cluster. For small clusters, Ca^{2+} sparks are short due to the influence of stochastic attrition. As RyRs increase in number for large clusters, increasingly rapid SR depletion underlies the shortening of the Ca^{2+} spark duration.

count for this difference. With more RyRs in a cluster, the total amount of Ca^{2+} released during a spark does not scale with the peak level of Ca^{2+} efflux due to the more rapid lumenal depletion, and the Ca^{2+} spark amplitude reflects the amount of Ca^{2+} bound to fluo-3, which is nonlinearly related to the total amount of Ca^{2+} released (Izu et al., 2001).

Figure 6 displays the composite results from 500 simulated Ca^{2+} sparks at each cluster size. The histograms displayed in Fig. 6 *A* demonstrate that, although the mean SR release duration remains relatively constant, as noted above, variability increases as the cluster size is decreased from 100 to 10 RyRs. Figure 6 *B* shows the less than proportional increase in Ca^{2+} spark amplitude, and Fig. 6 *C* displays the biphasic changes in SR release duration produced by increases in cluster size. Because of stochastic attrition, SR release is quite short for very small clusters, but SR release duration increases rapidly as stochastic attrition ceases to be a significant factor (e.g., with ~10 RyRs). With an increase in cluster size beyond ~20 RyRs, spark duration decreases slightly due to the faster SR depletion noted above.

With the parameters we have chosen for this model, the peak current through a single RyR (i.e., before local SR depletion occurs) is 0.07 pA. Although this is considerably smaller than any i_{RyR} that has been measured in bilayers, we feel that it may represent a realistic value for the single RyR current that occurs in cells (see Discussion). However, to ensure that these specific parameter choices did not significantly affect the overall model behavior, we ran additional simulations in which i_{RyR} was increased by a factor of 5, to 0.35 pA. Figure 7 compares the Ca^{2+} sparks observed with the control value of current (*A*) and with this increased value (*B*). With greater single-channel RyR Ca^{2+} flux, the peak Ca^{2+} release flux is larger, but SR depletion occurs more quickly, so the Ca^{2+} spark is not five times larger (similar to the changes that occur with increased RyR number). Interestingly, the SR release duration is almost identical even with this increased i_{RyR}. Thus, our model is robust enough that similar behavior occurs even with substantial changes in single-channel RyR current.

Effects of changes in $[Ca^{2+}]_{SS}$ and $[Ca^{2+}]_{lumen}$

As a test of the model, we examined how changes in $[Ca^{2+}]_{SS}$ and $[Ca^{2+}]_{lumen}$ affect simulated Ca^{2+} sparks. Because Ca^{2+} sparks are triggered by the large increase in $[Ca^{2+}]_{SS}$ resulting from a DHPR opening, smaller steady-state increases in global $[Ca^{2+}]_i$ will increase $[Ca^{2+}]_{SS}$. In the absence of Ca^{2+} spark triggering by the opening of

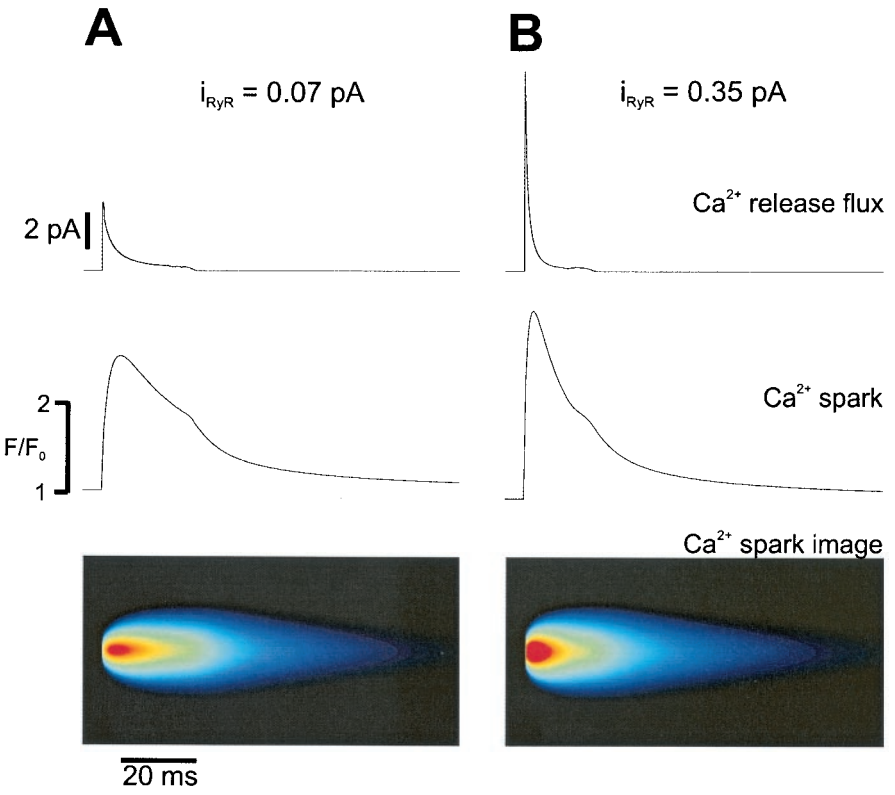

FIGURE 7 Effect of increasing single-channel RyR current. (*A*) Efflux from the subspace (*top*), F/F_0 0.25 μm from the source (*middle*), and simulated Ca^{2+} spark line-scan image (*bottom*) under control conditions, assuming a single-channel RyR current of 0.07 pA. (*B*) Simulated Ca^{2+} spark assuming an increased single-channel RyR current of 0.35 pA. Although the initial efflux is considerably larger, the Ca^{2+} spark amplitude is only larger by a factor of ~1.5. Ca^{2+} spark duration is almost identical.

DHPRs, this increase in $[Ca^{2+}]_{SS}$ will slightly increase the RyR opening rate and therefore should result in more frequent background or spontaneous sparks. Experimental studies have suggested (Cheng et al., 1996b) that such an increase in Ca^{2+} sparks occurs with elevated $[Ca^{2+}]_i$ (Satoh et al., 1997). We tested this idea by repeatedly running simulations with no DHPR opening and recording how often spontaneous Ca^{2+} sparks occurred. Figure 8, *A* and *B*, which displays simulated line-scan images that would be recorded from quiescent cells, shows that spontaneous sparks occur more frequently when $[Ca^{2+}]_{SS}$ is increased from 100 to 150 nM. On average (600 simulations, 800 ms each), this elevation in $[Ca^{2+}]_{SS}$ increased Ca^{2+} spark frequency by six times. Figure 8 *C* plots the spontaneous spark rate (defined as number of sparks per cluster per second) over a much wider range of intracellular Ca^{2+} concentrations. The Ca^{2+} spark rate increases by approximately four orders of magnitude as $[Ca^{2+}]_{SS}$ increases from 100 nM to ~1 μM.

Figure 9 *A* displays simulated Ca^{2+} sparks obtained at three different initial levels of $[Ca^{2+}]_{lumen}$. For these simulations, we fixed the network SR Ca^{2+} concentration at 1 mM to keep the $[Ca^{2+}]_{lumen}$ refilling rate relatively constant. Increasing the SR load increases the spark amplitude as one would expect but has little effect on Ca^{2+} spark duration. The SR Ca^{2+} fluxes that produce the sparks shown in Fig. 9 *A* are plotted on a normalized scale in Fig. 9 *B*. Consistent with experiments that back-calculated release flux from Ca^{2+} spark records (Lukyanenko et al., 1998), we observe an increase in the release flux decay rate with increasing SR load. Fig. 9, *C* and *D*, displays how changes in $[Ca^{2+}]_{lumen}$ affect the spontaneous spark rate and the spark duration, respectively. Spark rate is elevated nonlinearly with increasing $[Ca^{2+}]_{lumen}$, as experiments have demonstrated (Cheng et al., 1996b; Satoh et al., 1997). This increased occurrence of spontaneous sparks is thought to be responsible for the Ca^{2+} waves and arrhythmogenic currents that are seen in Ca^{2+} overload (E. A. Sobie, W. J. Lederer, and M. S. Jafri, work in progress). Ca^{2+} spark duration is extremely insensitive to $[Ca^{2+}]_{lumen}$ with refilling as we have modeled it. However, at extremely low SR Ca^{2+} loads, decreasing $[Ca^{2+}]_{lumen}$ further causes Ca^{2+} sparks to terminate prematurely.

In the absence of any dependence of RyR gating on $[Ca^{2+}]_{lumen}$, the model produces long Ca^{2+} sparks that do not terminate as illustrated in Fig. 10. Figure 10 shows how the composite P_o in the cluster changes (*A*) as the Ca^{2+} efflux (*B*) and $[Ca^{2+}]_{lumen}$ (*C*) decline. Panels *D* and *E* display the relative $[Ca^{2+}]$, 0.25 μm from the point of

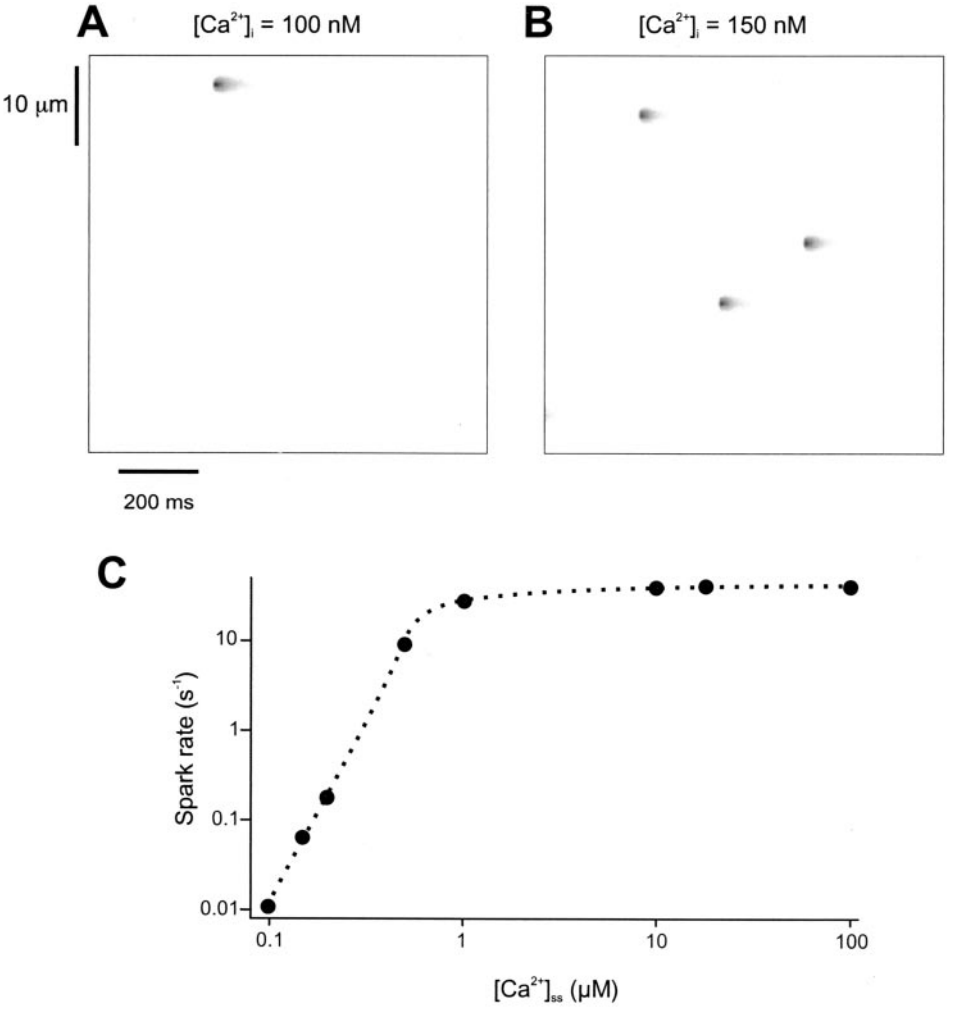

FIGURE 8 Effect of cytosolic $[Ca^{2+}]$ on spontaneous sparks. (*A*) Simulated Ca^{2+} line-scan image showing spontaneous sparks at cytosolic $[Ca^{2+}]$ of 100 nM. 600 simulations of 800 ms each were run without L-type channel openings to determine the rate at which spontaneous sparks occurred. The results of these simulations were translated into line-scan images by assuming that a longitudinal line scan that covered 50 μm of a ventricular myocyte would be able to detect Ca^{2+} sparks from 100 separate clusters of RyRs. (*B*) Simulated line-scan images showing spontaneous sparks with cytosolic $[Ca^{2+}]$ increased to 150 nM. More spontaneous sparks occur in this example. On average, the spontaneous spark rate was increased by six times upon increasing $[Ca^{2+}]_{SS}$ to 150 nM (5 spontaneous sparks in 4.8 s at $[Ca^{2+}]_i$ = 100 nM; 30 sparks at 150 nM). (*C*) Plot of normalized Ca^{2+} spark rate versus $[Ca^{2+}]_i = [Ca^{2+}]_{SS}$. The spontaneous spark rate (e.g., sparks per cluster per second) increases by four orders of magnitude as $[Ca^{2+}]_i$ increases from a resting level of 100 nM to 1 μM.

release and the line-scan image of the Ca^{2+} spark, respectively. The fluctuations in P_o during the Ca^{2+} spark arise because the decrease in $[Ca^{2+}]_{lumen}$ leads to a decrease in $J_{release}$ and hence a decrease in $[Ca^{2+}]_{SS}$. However, because RyR gating does not depend on $[Ca^{2+}]_{lumen}$, the fluctuations in P_o remain relatively minor, the RyRs are continually activated by the small but sustained $J_{release}$, and the Ca^{2+} spark does not terminate.

Stickiness of the RyRs in the cluster at the SR–TT junction

Because any specific assumption about the nature of RyR interactions in a cluster, other than their tendency to open and close together, would require arbitrary assumptions that would be difficult to verify experimentally (see Discussion), we modeled coupled gating of RyRs with the minimal number of assumptions. This allowed us to vary the strength of coupling between RyRs by modifying a single parameter, k_{coop} in Eq. 14. Figure 11 exhibits the changes in Ca^{2+} sparks that occur when k_{coop} is decreased from its control value of 1.0, reducing the tendency of one RyR to influence the P_o of another RyR. Typical Ca^{2+} sparks simulated with $k_{coop} = 0.5$ and $k_{coop} = 0.4$ are presented in Fig. 11, *A* and *B*, respectively. With decreased coupling between RyRs, there are large fluctuations in P_o. However, the coupling between channels is not strong enough for the closed channels to induce closure of the remaining channels while

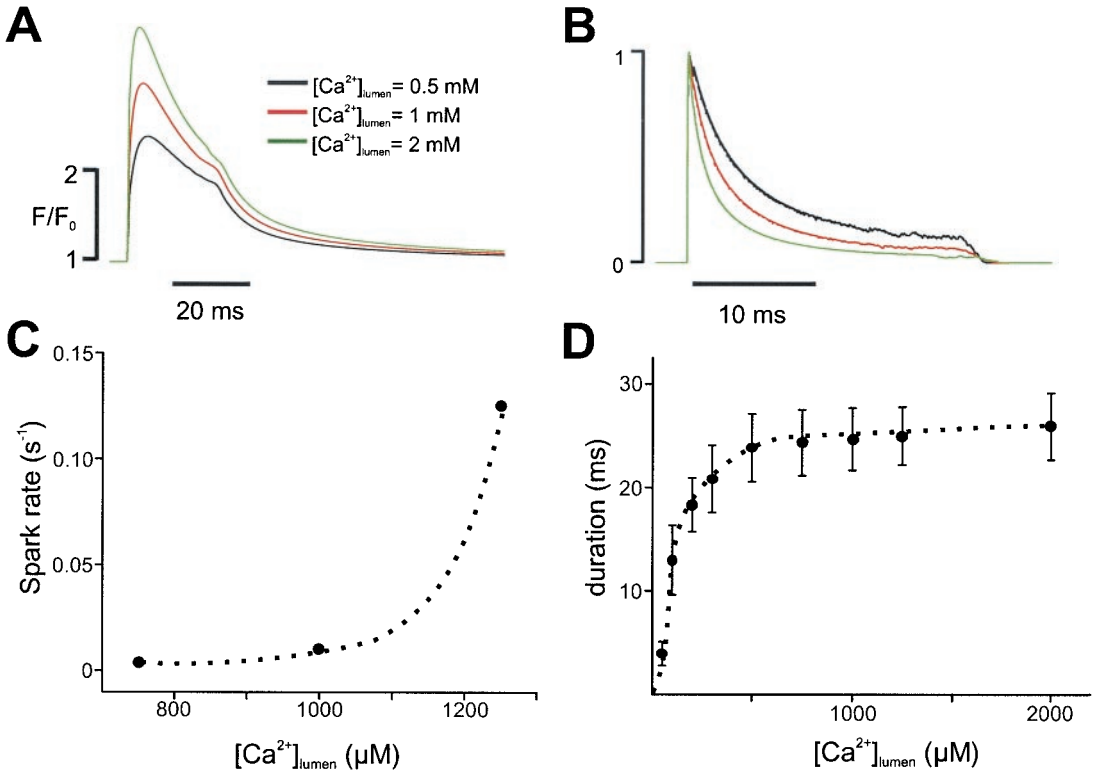

FIGURE 9 Effects of $[Ca^{2+}]_{lumen}$ on Ca^{2+} sparks. (*A*) Simulated Ca^{2+} sparks at different beginning levels of $[Ca^{2+}]_{lumen}$. With constant refilling rate, increasing $[Ca^{2+}]_{lumen}$ increases Ca^{2+} spark amplitude but does not change spark duration. (*B*) SR Ca^{2+} release fluxes that produce the sparks shown in (*A*), plotted on a normalized scale. Release flux decays more quickly with increased SR load. (*C*) Spontaneous spark rate increases nonlinearly with increases in $[Ca^{2+}]_{lumen}$. (*D*) Ca^{2+} release flux duration is generally insensitive to $[Ca^{2+}]_{lumen}$ except at extremely low SR load.

$[Ca^{2+}]_{SS}$ remains high. This leads to an increase in the duration of $J_{release}$, prolonged Ca^{2+} sparks, and noticeable fluctuations in fluorescence. Figure 12 *A* compares the durations of Ca^{2+} sparks for 500 simulations under control conditions ($k_{coop} = 1$, *left*) to those observed with decreased coupling ($k_{coop} = 0.4$, *right*). The duration of Ca^{2+} sparks (mean and standard deviation) is plotted against k_{coop} in Fig. 12 *B* over the range 0.4–1.5. The spark duration begins to rise rapidly, and variability increases, as k_{coop} declines to values less than ~0.7. When coupling between RyRs is removed completely ($k_{coop} = 0$), Ca^{2+} sparks do not terminate (data not shown), revealing Ca^{2+} sparks that look roughly like the one shown in Fig. 10. Due to the maintained dependence on $[Ca^{2+}]_{lumen}$, there are greater fluctuations in P_o. However, in the absence of coupled gating, the activation of RyRs in the cluster is sufficient to produce a maintained Ca^{2+} spark.

FK506 and Rapamycin

Because FK506 and rapamycin have been shown to reduce coupled gating between RyRs in planar lipid bilayer experiments (Marx et al., 2001), but conflicting effects on Ca^{2+} sparks in intact heart cells have been reported, (McCall et al., 1996; Xiao et al., 1997), we carried out experiments in mouse heart cells. Consistent with some prior reports (Xiao et al., 1997; Lukyanenko et al., 1998) we observed prolonged Ca^{2+} sparks in the presence of FK506 or rapamycin as shown in Fig. 13. Figure 13 *D* shows that about half of the Ca^{2+} sparks obtained in FK506 lasted longer than 40 ms, whereas only ~10% of control Ca^{2+} sparks did. These findings are consistent with the hypothesis that RyR interactions, including those involving RyR-associated proteins like FKBP12.6, contribute to Ca^{2+} spark termination. Other actions of FK506 and related agents are discussed below.

DISCUSSION

Overview

We have developed a relatively simple mathematical model of the cardiac Ca^{2+} spark to test a new hypothesis that addresses one of the remaining major unresolved questions in cardiac EC coupling: how Ca^{2+} sparks are able to terminate. In the model, a cluster of up to a hundred RyRs in an SR junction is responsible for a Ca^{2+} spark, and the RyR Ca^{2+} release channels can assume only one of two conformations: open or closed. However, each RyR is influenced by the ensemble

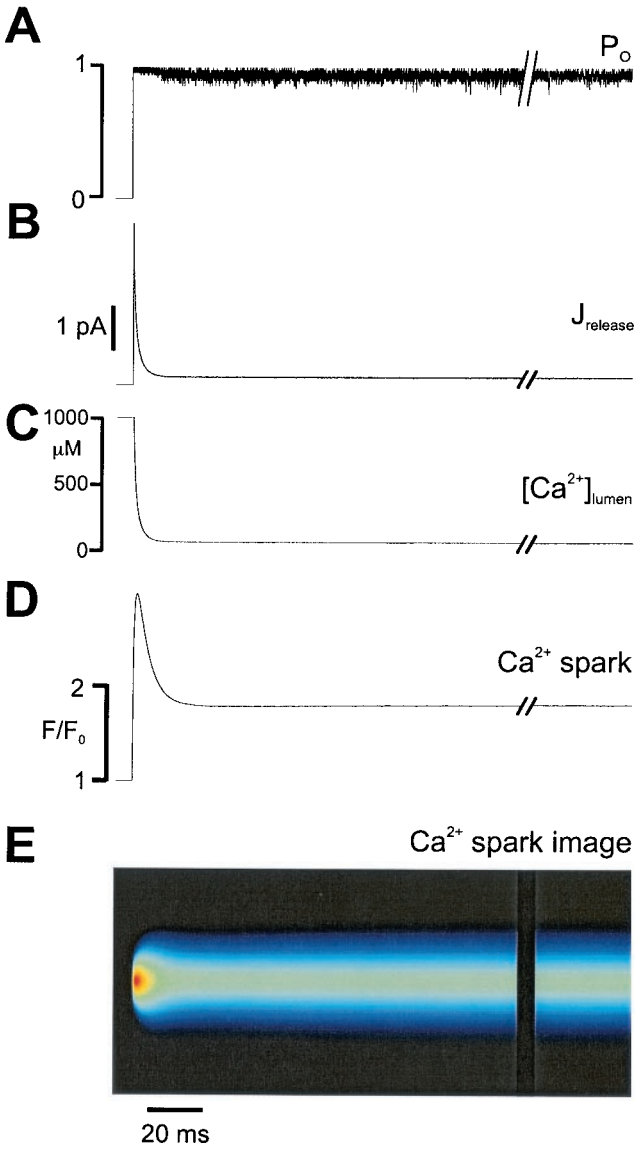

FIGURE 10 Ca^{2+} sparks when $[Ca^{2+}]_{lumen}$ has no effect on RyR gating. (*A*) Composite RyR P_o versus time. For this simulation, K_m in Eq. 3 was set to 3.6 μM, the value at the control diastolic $[Ca^{2+}]_{lumen}$ of 1 mM. Release does not terminate before the end of the 800-ms simulation and was not observed under these conditions. (*B*) $J_{release}$. (*C*) $[Ca^{2+}]_{lumen}$. (*D*) $[Ca^{2+}]_i$ as F/F_0 (0.25 μm from source). (*E*) Line-scan image of Ca^{2+} spark. Note that, during the prolonged spark, F/F_0 is maintained at ~60% of its peak level, although the release flux declines by more than 90%. This occurs because of the presence of cytosolic Ca^{2+} buffers.

behavior of the other RyRs in the cluster through a cooperativity factor (k_{coop}) thereby allowing the model to simulate coupled gating among RyRs. We term this the sticky cluster model to emphasize the central importance of physical contact between neighboring RyRs. The other key feature of the model is that RyR gating is influenced not only by the local cytosolic $[Ca^{2+}]$ in the subspace ($[Ca^{2+}]_{SS}$), but also by the Ca^{2+} concentration in the local JSR lumen ($[Ca^{2+}]_{lumen}$). The combination of these two factors provides the negative feedback and hysteresis that allow for Ca^{2+} sparks to terminate robustly and not be immediately re-triggered. The model thus takes into account new findings on both the anatomy and the gating behavior of cardiac RyRs.

The sticky cluster model successfully reproduces many features of cardiac Ca^{2+} sparks and is consistent with simple experimental interventions. Model Ca^{2+} sparks terminate readily, and many features of Ca^{2+} sparks are largely insensitive to the number of RyRs in the cluster (Figs. 5 and 6). In addition, increases in either $[Ca^{2+}]_{SS}$ or $[Ca^{2+}]_{lumen}$ increase the frequency with which spontaneous sparks occur (Figs. 8 and 9), as experiments have shown (Cheng et al., 1996b; Satoh et al., 1997; Lukyanenko et al., 2001). Finally, decreasing coupling between RyRs prolongs Ca^{2+} spark duration (Fig. 12), similar to the experimental effects of FK506 (Fig. 13). The model should therefore prove useful for generating new predictions and extending our understanding of Ca^{2+} signaling in heart. The work does, nevertheless, raise some specific points of interest that can only be addressed with additional experiments and computer modeling.

Termination of Ca^{2+} sparks

As a high-gain, positive-feedback system, CICR is potentially unstable. One way that the cardiac myocyte minimizes the risk of instability is by placing CICR under local control. By this it is meant that the Ca^{2+} transient reflects the recruitment of individual units of release (Ca^{2+} sparks), which are triggered by local increases in Ca^{2+} and do not themselves trigger regenerative, cell-wide Ca^{2+} release under normal conditions. However, the stability provided by local control would be lost without a reliable mechanism for the termination of Ca^{2+} sparks.

Three primary explanations for how Ca^{2+} sparks terminate have been proposed in the literature. First, it is possible that the SR exhausts its supply of Ca^{2+}, and the duration of a Ca^{2+} spark reflects the time it takes to empty the local SR Ca^{2+} store. This explanation appears unlikely because the SR retains much Ca^{2+} after a $[Ca^{2+}]_i$ transient (Varro et al., 1993; Negretti et al., 1995; Bassani et al., 1995) and because extremely long (seconds) Ca^{2+} sparks can be observed under certain experimental conditions (Cheng et al., 1993). Second, it is possible that the RyRs undergo Ca^{2+}-dependent or use-dependent inactivation after they open. However, in planar lipid bilayer experiments, simple steady-state inactivation only occurs at Ca^{2+} concentrations above ~10 mM (Sitsapesan and Williams, 2000) not at the concentrations that are thought to be present near the RyRs during a Ca^{2+} spark (10–100 μM) (Meissner et al., 1988; Rousseau and Meissner, 1989; Ashley and Williams, 1990). RyRs in bilayer experiments display adaptation (a complicated form of inactivation), but this process is incomplete and occurs relatively slowly (Györke and Fill, 1993; Valdivia et al., 1995). These observations argue against a primary role for adaptation or inactivation in the termination of Ca^{2+} sparks.

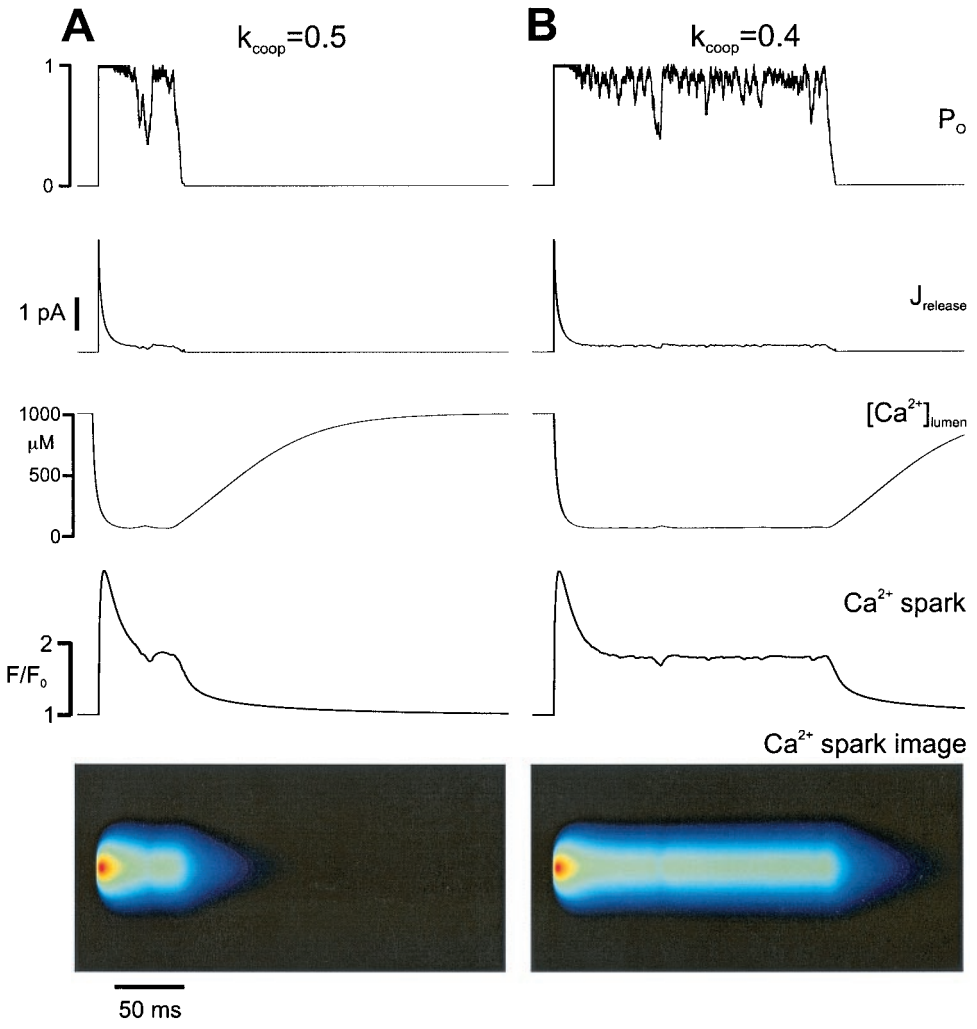

FIGURE 11 Ca^{2+} sparks under conditions of reduced coupling between RyRs. Time course of Ca^{2+} spark components when coupling between RyRs is reduced. (*A*) Reduced coupled gating with $k_{coop} = 0.5$. P_o (*top*), $J_{release}$ (*second from top*), $[Ca^{2+}]_{lumen}$ (*middle*), $[Ca^{2+}]_i$ as F/F_0 (0.25 μm from source, *second from bottom*), and line-scan image of Ca^{2+} spark (*bottom*). (*B*) Reduced coupled gating with $k_{coop} = 0.4$. The release flux lasts for ~60 ms ($k_{coop} = 0.5$) and ~200 ms ($k_{coop} = 0.4$), leading to prolonged Ca^{2+} sparks. Reduced coupling also leads to increased flickering of RyRs during the prolonged release, which is apparent in the spark time course and image. These fluctuations vary greatly from simulation to simulation as does the Ca^{2+} spark duration (see Fig. 12).

A third possibility is "stochastic attrition" (Stern, 1992), whereby all of the RyRs in a cluster happen to close at the same time. Although this would be a plausible hypothesis if very small RyR clusters produced Ca^{2+} sparks, stochastic attrition becomes increasingly unlikely as the number of RyRs in a cluster increases (Stern, 1992; Stern et al., 1999) and its probability is vanishingly small when more than ~20 RyRs are present.

The model presented here overcomes the limitations of other hypotheses while incorporating some of their important features. Our proposed mechanism is similar to stochastic attrition in the sense that some RyRs must close probabilistically for coupled gating to induce the remaining channels to close. It resembles SR exhaustion in that substantial local SR depletion is required for the spark to terminate. We modeled RyR gating without any inactivation or adaptation processes to demonstrate that these are not necessary for Ca^{2+} spark termination, but these results do not necessarily argue against an important role for either of these mechanisms in the regulation of cardiac CICR. Adding either of these phenomena to the model would presumably assist the termination of the Ca^{2+} spark by closing some of the RyRs in the cluster, thus causing the SR release flux to decay more steeply and subspace $[Ca^{2+}]$ to be reduced. Finally, coupled gating as we have modeled it is similar in spirit to the allosteric interactions between RyRs that have been modeled by Stern et al. (1999). However, although allosteric interactions could greatly stabilize the activation of Ca^{2+} release in that model, their effects on termination of release were less well-explored and only occurred through the transition to an inactivated state. Additional work is clearly necessary to better explore the

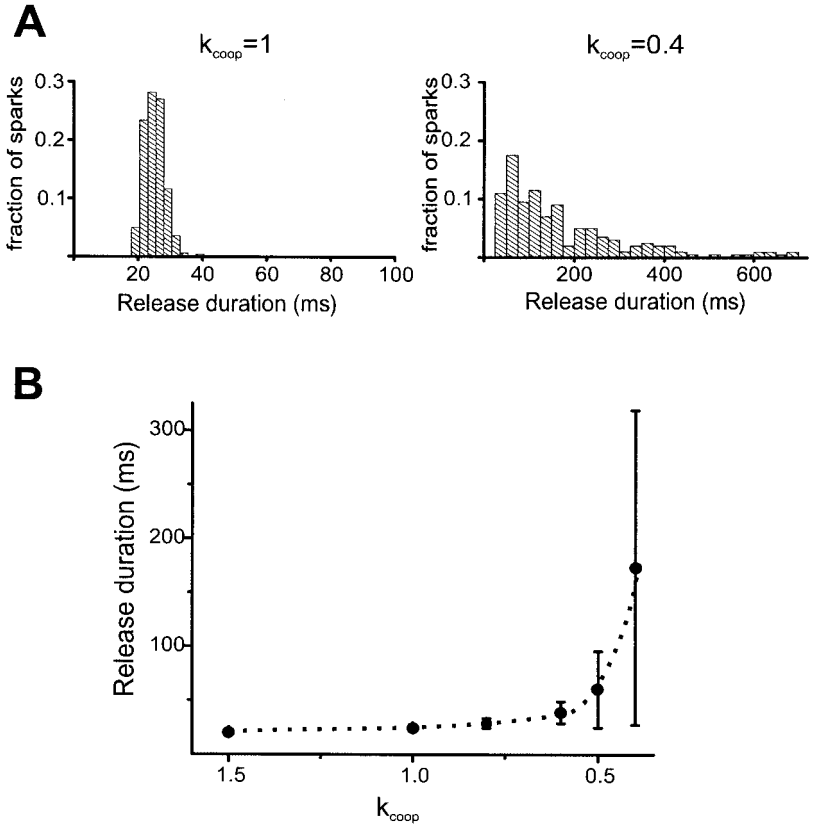

FIGURE 12 Ca^{2+} spark duration when RyR coupling is reduced. (*A*) Histograms of Ca^{2+} release duration generated by 500 simulations with k_{coop} = 1 (control conditions, *left*) and k_{coop} = 0.4 (*right*). Bins are 2.5 ms wide for control and 25 ms wide for k_{coop} = 0.4. (*B*) Mean release duration and standard deviation (error bars) versus decreasing strength of coupling (k_{coop}). Reducing the coupling between RyRs greatly increases both the mean value and the variability of the Ca^{2+} spark duration.

multiple effects that interactions between RyRs can have on cluster behavior.

Restitution and SR Ca^{2+} content

Following a Ca^{2+} release event, time must elapse before CICR can be triggered again, at both the local (Ca^{2+} spark) and global (cell-wide Ca^{2+} transient) levels, a feature called "restitution." For instance, a Ca^{2+} transient evoked by field stimulation after a spontaneous Ca^{2+} wave caused less Ca^{2+} release in locations that the wave had just passed than in locations at which more time had elapsed (Cheng et al., 1996b). Consistent with this, Tanaka et al. (1998) found that, during a Ca^{2+} transient, sparks were not triggered at locations where a spontaneous Ca^{2+} spark had occurred within the previous 25 ms. In addition, Sham et al. (1998) observed a negative correlation between the amounts of Ca^{2+} release triggered by Ca^{2+} current upon depolarization and by Ca^{2+} tail current upon repolarization. In other words, sites that released Ca^{2+} early during a depolarizing pulse tended to not release Ca^{2+} when a second Ca^{2+} influx occurred at the end of the pulse, even though the SR still contained Ca^{2+} (Sham et al., 1998). Although these results can be interpreted to indicate a refractoriness of Ca^{2+} release due to Ca^{2+}-dependent or use-dependent inactivation, it is also possible that this refractoriness results from the time it takes for partially depleted SR release sites to be refilled with Ca^{2+}. If RyRs are more likely to open when $[Ca^{2+}]_{lumen}$ is high, as we have modeled here and as experiments have indicated, Ca^{2+} sparks will be more difficult to trigger during the refilling time that follows a spark. This factor makes it difficult to interpret experiments in which the cell contains a high concentration of exogenous intracellular Ca^{2+} buffer, because these buffers compete with the SR Ca^{2+} pump and slow reuptake of Ca^{2+} into the SR (Sham et al., 1998; DelPrincipe et al., 1999). Indeed, studies that have used high Ca^{2+} buffer concentration have observed an unrealistically slow recovery of Ca^{2+} release (DelPrincipe et al., 1999). Clearly more experiments are necessary to resolve the roles played by SR refilling, recovery from inactivation, and possibly other mechanisms in the restitution process.

What is the shape of the Ca^{2+} release flux?

Most previous models of the cardiac Ca^{2+} spark (see below), have, for simplicity, assumed that a spark results from

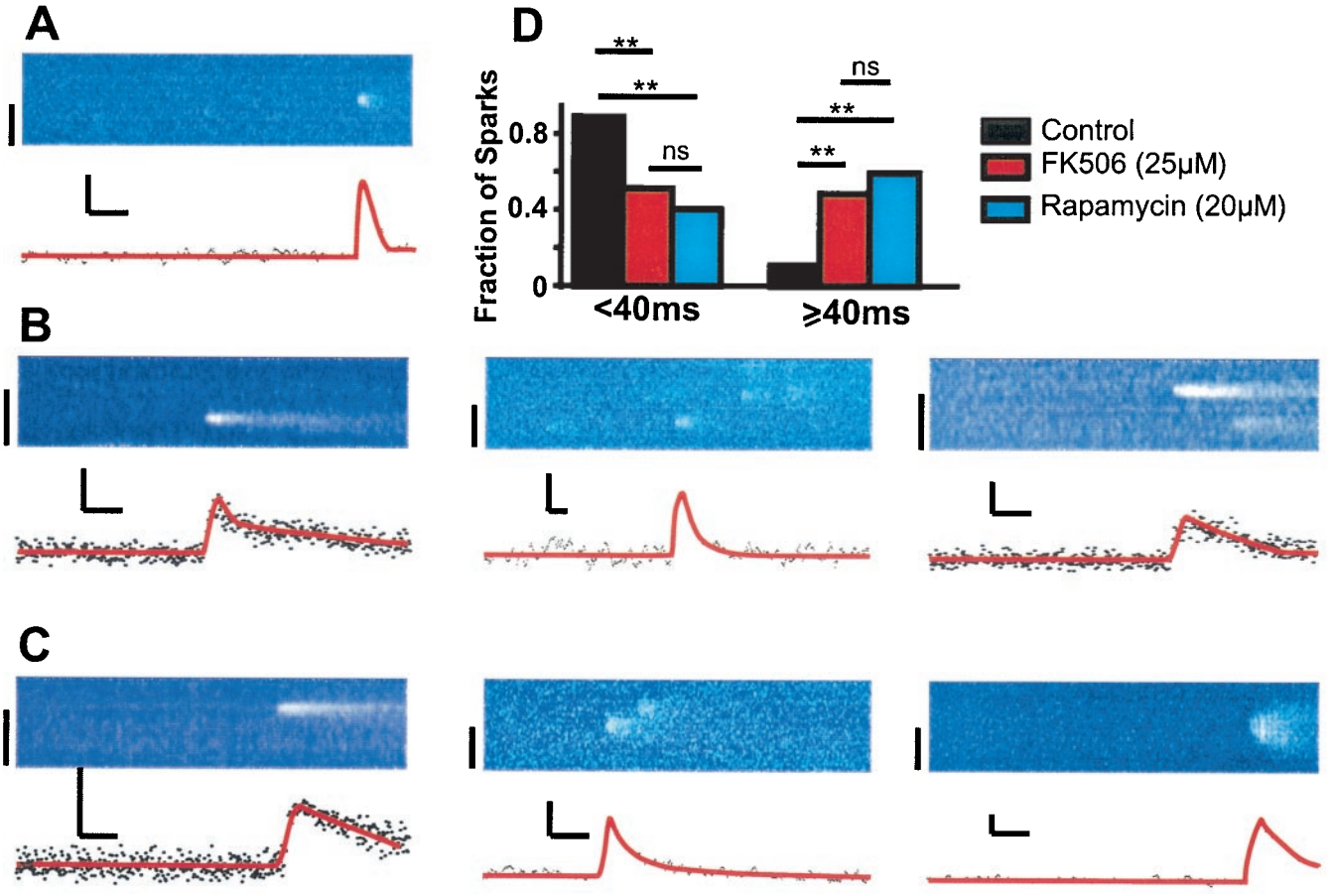

FIGURE 13 Experimental results: effects of FK506 and rapamycin. (*A*) A typical Ca^{2+} spark (line-scan image: position shown vertically, time horizontally) under control conditions (*top*), and plot of F/F_0 (*bottom*). (*B*) Three examples of Ca^{2+} sparks following application of 25 μM FK506 displayed as in (*A*). (*C*) Three examples of Ca^{2+} sparks following application of 20 μM rapamycin displayed as in (*A*). (*D*) Fraction of total Ca^{2+} sparks <40 ms and ≥40 ms. ** $p < 0.05$. Calibration: position = 10 μm; fluorescence = 0.5 F/F_0; time = 100 ms.

a constant SR Ca^{2+} release flux. In skeletal muscle, Schneider and colleagues have used curve-fitting of high temporal resolution Ca^{2+} spark recordings to argue that the Ca^{2+} release flux underlying the Ca^{2+} spark is constant (Lacampagne et al., 1999), but a comparable study on cardiac Ca^{2+} sparks has not yet been done. For a variety of reasons, we believe that the cardiac Ca^{2+} spark likely results from a decaying SR Ca^{2+} release flux. First, the extremely small volume of the junctional SR suggests that, even with considerable Ca^{2+} buffering power, Ca^{2+} release through a cluster of RyRs could empty this volume rather quickly. For example, a local JSR with a diameter of 300 nm and a depth of 10 nm would have a volume of only 7×10^{-4} μm^3 (assuming a cylindrical geometry). Even with 50 mM of buffer-bound Ca^{2+} and 1 mM free Ca^{2+}, this volume wound only contain ~21000 Ca^{2+} ions. Because a 1-pA current is equivalent to ~3000 Ca^{2+} ions per millisecond, the Ca^{2+} in the local JSR would only be able to provide the Ca^{2+} spark release flux a few milliseconds. Thus, even if refilling of the JSR is fast, it seems likely that significant local SR depletion could occur over the time scale of the Ca^{2+} spark.

The idea of a decaying release flux accounting for the cardiac Ca^{2+} spark is consistent with the results of Lukyanenko et al. (1998), who back-calculated the responsible fluxes from line-scan Ca^{2+} spark recordings. However, the accuracy of their calculations could have been compromised by the simple buffering approximation that they used. They assumed, as we have here, that binding of fluo-3 to stationary cytoplasmic proteins can be modeled by simply reducing the fluo-3 diffusion constant. However, the results of Harkins et al. (1993) suggest that fluo-3 bound to Ca^{2+} has a different affinity for proteins than does free fluo-3. For this reason, we performed additional simulations with a more complex buffering-diffusion scheme derived from the Harkins et al. data (detailed in Hollingworth et al., 2000). The Ca^{2+} sparks produced by stereotyped Ca^{2+} release fluxes with the complex buffering scheme are compared with those generated with the simple buffering scheme (i.e., the model used in the other simulations) in Fig. 14. Three

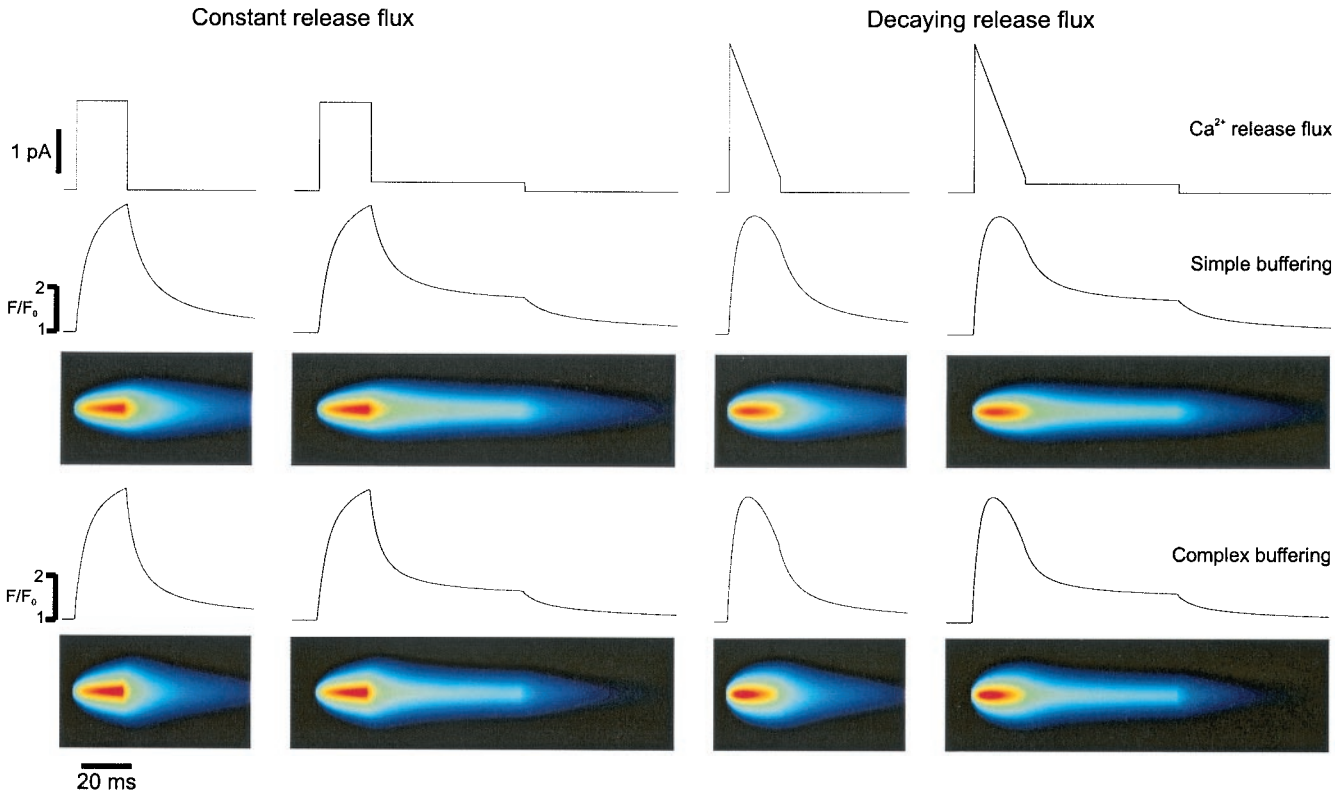

FIGURE 14 Effects of diffusion-buffering model on Ca^{2+} spark characteristics. Ca^{2+} sparks produced by stereotyped Ca^{2+} release fluxes (*top*) were computed with both the simple buffering and the complex buffering approximations (see text for descriptions). The middle panels present the Ca^{2+} spark time course (0.25 μm from the source) and line-scan image for simple buffering, whereas the bottom panels display these for complex buffering.

features of these simulations are of interest. One is that Ca^{2+} sparks produced by decaying fluxes are rounded at the peak, whereas those resulting from constant fluxes come to a sharp peak when release shuts off. A second observation is that the choice of buffer model causes only subtle changes in the Ca^{2+} spark shape. In other words, the Ca^{2+} spark time courses produced by constant and decaying sources look similar with either buffer model. Finally, the extended Ca^{2+} sparks displayed show that a maintained flux of only10% of the peak level can produce a maintained $\Delta F/F_0$ of ~50% of the peak level. These maintained F/F_0 levels, which are similar to those observed experimentally (e.g., Fig. 13), suggest that a very small Ca^{2+} flux can maintain a significant plateau during long Ca^{2+} sparks. Because of the presence of slow Ca^{2+} buffers in the Ca^{2+} spark model, the peak $\Delta F/F_0$ that is achieved during the ~20 ms of release in the normal Ca^{2+} spark is considerably less than the steady-state level that would be achieved if this flux were maintained indefinitely. Thus, a small maintained flux can produce a relatively larger $\Delta F/F_0$. Simulated sparks in which the maintained flux was 50% of the peak produced Ca^{2+} sparks with plateau levels close to the peak levels, inconsistent with the experimental data (results not shown). Taken together, these observations strongly suggest cardiac Ca^{2+} sparks result from Ca^{2+} release fluxes that decay with time. However, because flux depends on both the RyR open probability and the Ca^{2+} gradient, a decay in the release flux can theoretically result from severe local depletion, as we have modeled here, from strong inactivation of RyRs, or from a combination of the two.

Other spark models

Earlier models of the Ca^{2+} release process (Stern, 1992; Stern et al., 1999; Rice et al., 1999) or Ca^{2+} spark characteristics (Pratusevich and Balke, 1996; Smith et al., 1998; Izu et al., 2001) have provided useful interpretations of experimental data and predictions that have motivated important new experiments. Our results complement these studies by examining issues that earlier models did not thoroughly address. Specifically, our study extends previous work in the following ways: 1) the model provides a hypothesis for the termination of Ca^{2+} release that is experimentally justified; 2) simple experimental interventions have been modeled and are consistent with published data; 3) Ca^{2+} spark properties are maintained roughly the same when the RyR number is varied; and 4) the Ca^{2+} sparks produced by our release fluxes are rounded at their peak rather than coming to a sharp peak (Smith et al., 1998) or having a flat-top shape (Izu et al., 2001). However, one weak-

ness of the previous studies, which is shared by models of skeletal muscle Ca^{2+} sparks (Jiang et al., 1999), has not been overcome in the present model: Ca^{2+} spark width (full-width at half-maximum (FWHM) is about half of that observed experimentally. This is due in part to the way that fluo-3 diffusion was modeled with the simple buffering scheme, because sparks simulated with the complex buffering scheme (Fig. 14) are somewhat wider (FWHM at the peak 1.39 versus 1.32 μm). It is also interesting to note that Ca sparks with a decaying release flux have larger FWHM than those produced by the equivalent constant release flux (e.g., 1.66 μm in the Smith buffering model). However, simulated sparks still have a smaller FWHM than that observed experimentally. Another hypothesis for the unreasonable narrowness of model Ca^{2+} sparks is that the fluxes thought to produce sparks are too small by approximately an order of magnitude (Izu et al., 2001). More experiments and modeling will be necessary to test this provocative idea.

Relationship to RyR gating in planar lipid bilayers

To explore easily the mechanisms by which Ca^{2+} release terminated in the model, we implemented a simple RyR gating scheme that did not include features explored in other studies (e.g., adaptation, inactivation, or modal gating). Thus, detailed comparisons between these models of RyR gating and our integrated model of Ca^{2+} spark behavior are impossible. We can, however, compare our results to other published RyR schemes in terms of sensitivity to activation by subspace $[Ca^{2+}]$. In the absence of coupled gating in our model and with 1 mM $[Ca^{2+}]_{lumen}$, a single RyR tetramer displays half-maximal activation at 1.28 μM, which is similar to the sensitivity (0.6 μM) of the relatively simple scheme of Cannell and Soeller (1997). Without running extensive simulations, it is not straightforward to compute half-maximal activation in more complex models, but the fact that other models (Zahradnikova and Zahradnik, 1996; Keizer and Smith, 1998; Fill et al., 2000) show activation of RyRs by steps of Ca^{2+} to 1 μM indicates that these models have similar sensitivity to $[Ca^{2+}]_{SS}$ as ours. However, we should note that, because RyRs are involved in the locally positive-feedback process of CICR, in both our integrated model and in cells, more than just the equilibrium values of Ca^{2+} activation are important. A small initial RyR opening can increase $[Ca^{2+}]_{SS}$ and increase the open probability of the other channels in the cluster (even without coupled gating), which means that the dynamics of RyR opening will be extremely important in determining how Ca^{2+} sparks are triggered and terminate. In addition, factors such as Mg^{2+}, ATP, and phosphorylation by cellular kinases can influence RyR gating, but our understanding of these effects is still incomplete. Despite these limitations, we feel that our gating scheme is consistent with critical features of RyR behavior.

RyRs, sticky clusters, and spatial organization with the heart cell

The large number of RyRs in a cluster in heart (Franzini-Armstrong et al., 1998, 1999) along with evidence of coupled gating among RyRs in heart (Marx et al., 2001) suggests that sticky clusters may be functionally important. The two-dimensional organization of such clusters would depend on how they were arranged with respect to the TT and the size of the TTs at the SR–TT junction. Current estimates are that TTs in mammalian hearts are ~300 nm in diameter, permitting a half-circumference of ~500 nm. If RyRs were spaced 50 nm apart within a cluster, such a TT could readily accommodate a cluster of 100 RyRs arranged in a square symmetrical array. If each cluster contained 100 RyRs and the cell contained 10^6 total RyRs, the clusters would be separated by 2 μm in the longitudinal direction and 1 μm along the other directions, assuming a cell size of 200 $\times$ 20 $\times$ 10 μm. A 1-μm-thick image would therefore contain 10 clusters per Z line. If each cluster contained fewer RyRs, this would require closer spacing between clusters and a greater number of Ca^{2+} spark sites. These issues become extremely important when exploring how restitution occurs and how Ca instability arises, which is why morphometry data that examines this organization and new experiments that examine functional characteristics of the SR will be invaluable in advancing our understanding of calcium signaling in heart.

Here we should note that it is possible that some of the RyRs present in a cluster are inactive and do not contribute to the release flux that produces a Ca^{2+} spark. We think it is one of the major strengths of the model that robust termination, and relatively constant Ca^{2+} spark characteristics, occur for RyR clusters of various sizes. Thus, if a particular cluster contained 100 RyRs, the same general mechanism for spark termination could be operable whether all 100 or only 20 of those channels were active. As new information becomes available, we may need to adjust model parameters, such as the strength of coupling between RyRs, the single channel RyR conductance, or the lumenal dependence of RyR gating to simulate accurately the detailed characteristics of Ca^{2+} sparks. However, the general mechanism we have proposed here should still provide robust termination of Ca^{2+} release and realistic Ca^{2+} sparks.

Model choices

Because our aim was to incorporate the most recent experimental observations into our new Ca^{2+} spark model, we simulated phenomena that are incompletely characterized and were therefore forced to make certain somewhat arbitrary choices. The reasons for some of our choices, and how the model may need to be adjusted as new data become available, are detailed here.

It is unclear exactly how many RyRs are present in each cluster, and this number may be species-dependent (Franzini-Armstrong et al., 1998, 1999). Although we defined a control cluster as containing 50 RyRs, we consider it a strength of the model that Ca^{2+} spark duration is relatively insensitive to the number of RyRs in the cluster. However, as additional morphological data become available, parameters such as RyR number, single RyR Ca^{2+} flux, and the strength of coupling between RyRs may need to be modified for the model to produce realistic sparks. The value that we chose for i_{RyR}, 0.07 pA, is smaller than any single channel RyR current that has been measured experimentally, but we feel it may be a realistic estimate of the physiological RyR flux. Our parameters were based on the single channel bilayer study of Mejia-Alvarez et al. (1999) under quasi-physiological conditions but were adjusted to account for the slightly different ionic conditions that we modeled. These authors recorded an i_{RyR} of 0.35 pA with 150 mM cytosolic Cs^+, 0 mM cytosolic Mg^{2+}, and 2 mM lumenal Ca^{2+} (their Fig. 2). If we adjust for the smaller current that would be present with 1 mM lumenal Ca^{2+}, and for the ~67% reduction in current caused by 1 mM Mg^{2+} (as in their Fig. 5), this yields approximately 0.07 pA, close to the value we used. A similar result is obtained by linear interpolation of their Fig. 6 *A* to account for the different conditions present.

The notion that lumenal Ca^{2+} affects RyR gating, although initially controversial, is now supported by both indirect evidence from cellular studies of CICR and direct evidence from bilayer studies. However, it remains uncertain whether this effect is mediated through free Ca^{2+} in the lumen or through Ca^{2+} binding to an associated protein such as calsequestrin. Thus, our mathematical representation of this effect should not be considered unique. Indeed, in preliminary simulations, we were able to produce Ca^{2+} release fluxes that decayed much less severely but still terminated robustly by varying the sensitivity of RyR gating to $[Ca^{2+}]_{lumen}$ and the rate of JSR refilling (results not shown). Also, although the Marks (1996) lab has observed coupled gating between both skeletal muscle (Marx et al., 1998) and cardiac (Marx et al., 2001) RyRs, these results have not yet been confirmed by others and remain controversial. This discrepancy probably results from slight differences in the experimental protocols used to isolate RyRs for bilayer studies and emphasizes that caution needs to be exercised when interpreting behavior of ion channels observed under conditions far from their native state. Finally, because there is not enough experimental data currently available to provide an accurate mathematical representation of coupled gating, we decided to simplify our modeling of coupled gating by not considering any spatially resolved interactions between RyRs. Although this representation has proven to be adequate for the present considerations, it is undoubtedly an oversimplification, and a more complex treatment may be necessary to examine phenomena such as restitution or how Ca^{2+} sparks produce Ca^{2+} waves. One possible approach is suggested by modeling of conformational spread in clusters of receptors involved in bacterial chemotaxis. This formulation, in which the presence of a receptor in one state makes that state more energetically favorable for the neighboring receptors, has been shown to influence the behavior of clusters in several potentially useful ways (e.g., greater sensitivity) (Duke and Bray, 1999; Duke et al., 2001). In general, then, the broad outlines of our model are clearly consistent with the majority of the experimental data available, but several minor adjustments will likely need to be made as these phenomena are characterized in greater detail.

FKBP/FK506/Rapamycin

FK506 has been shown to bind to FKBP12.6 and FKBP12 and remove them from the RyRs to which they are associated (Marks, 1996; Yano et al., 2000; Marx et al., 2000, 2001; Bultynck et al., 2001; Prestle et al., 2001). The application of FK506 reversibly disrupts coupled gating over time in planar lipid bilayer experiments. In experiments on isolated cells, FK506 has been shown by others (Xiao et al., 1997; Lukyanenko et al., 1998) to cause long Ca^{2+} sparks similar to those presented here (Fig. 13), but one group reported no change in Ca^{2+} spark characteristics (McCall et al., 1996). This conflicting observation may result from the fact that Ca^{2+} spark half-amplitude durations were reported by McCall et al. (1996). With such a definition of Ca^{2+} spark duration, sparks that decline to a plateau level below 50% of the peak and are then extended would not be considered to be longer than normal. The collection of data thus suggests that the proposed model is reasonable. However it should be noted that FK506 and rapamycin have additional effects on cellular function (duBell et al., 1997, 1998, 2000), but the effect they have in common is to bind FKBPs and change RyR behavior.

CONCLUSIONS

We have proposed a new model of the cardiac Ca^{2+} release process in which a Ca^{2+} spark results from the action of a sticky cluster of RyRs. It succeeds in characterizing this high-gain, positive-feedback CICR signaling system under many conditions. Although experimental results obtained to date are consistent with the model, many features of Ca^{2+} signaling have not yet been tested or investigated. Similarities in other CICR systems may enable modified versions of the model of Ca^{2+} spark behavior to be applied to smooth muscle and skeletal muscle.

We would like to thank Dennis Bray for discussion and comments, Greg Smith for code sharing and discussion on modeling of Ca^{2+} sparks, and Andrew R. Marks for discussion on coupled gating. We would also like to thank the reviewers of the manuscript for useful suggestions.

Support is acknowledged from National Institutes of Health (W.J.L.), and the National Institutes of Health-supported training programs in Muscle Biology (E.A.S.) and Membrane Physiology (K.W.D.).

REFERENCES

Ashley, R. H., and A. J. Williams. 1990. Divalent cation activation and inhibition of single calcium release channels from sheep cardiac sarcoplasmic reticulum. *J. Gen. Physiol.* 95:981–1005.

Bassani, J. W. M., W. Yuan, and D. M. Bers. 1995. Fractional SR Ca release is regulated by trigger Ca and SR Ca content in cardiac myocytes. *Am. J. Physiol. Cell Physiol.* 268:C1313–C1319.

Bhat, M. B., J. Zhao, W. Zang, C. W. Balke, H. Takeshima, W. G. Wier, and J. Ma. 1997. Caffeine-induced release of intracellular Ca^{2+} from Chinese hamster ovary cells expressing skeletal muscle ryanodine receptor. Effects on full-length and carboxyl-terminal portion of Ca^{2+} release channels. *J. Gen. Physiol.* 110:749–762.

Bultynck, G., P. De Smet, D. Rossi, G. Callewaert, L. Missiaen, V. Sorrentino, H. De Smedt, and J. B. Parys. 2001. Characterization and mapping of the 12 kDa FK506-binding protein (FKBP12)-binding site on different isoforms of the ryanodine receptor and of the inositol 1,4,5-trisphosphate receptor. *Biochem. J.* 354:413–422.

Cannell, M. B., H. Cheng, and W. J. Lederer. 1994. Spatial non-uniformities in $[Ca^{2+}]_i$ during excitation–contraction coupling in cardiac myocytes. *Biophys. J.* 67:1942–1956.

Cannell, M. B., H. Cheng, and W. J. Lederer. 1995. The control of calcium release in heart muscle. *Science.* 268:1045–1050.

Cannell, M. B. and C. Soeller. 1997. Numerical analysis of ryanodine receptor activation by L-type channel activity in the cardiac muscle diad. *Biophys. J.* 73:112–122.

Cannell, M. B., and C. Soeller. 1999. Mechanisms underlying calcium sparks in cardiac muscle. *J. Gen. Physiol.* 113:373–376. [Erratum. *J. Gen. Physiol.* 1999, 113:761].

Cheng, H., M. B. Cannell, and W. J. Lederer. 1994. Propagation of excitation–contraction coupling into ventricular myocytes. *Pflügers Arch.* 428:415–417.

Cheng, H., M. R. Lederer, R.-P. Xiao, A. M. Gómez, Y.-Y. Zhou, B. Ziman, H. Spurgeon, E. G. Lakatta, and W. J. Lederer. 1996a. Excitation–contraction coupling in heart: new insights from Ca^{2+}-sparks. *Cell Calcium.* 20:129–140.

Cheng, H., M. R. Lederer, W. J. Lederer, and M. B. Cannell. 1996b. Calcium sparks and $[Ca^{2+}]_i$ waves in cardiac myocytes. *Am. J. Physiol. Cell Physiol.* 270:C148–C159.

Cheng, H., W. J. Lederer, and M. B. Cannell. 1993. Calcium sparks: elementary events underlying excitation–contraction coupling in heart muscle. *Science.* 262:740–744.

Ching, L. L., A. J. Williams, and R. Sitsapesan. 2000. Evidence for Ca^{2+} activation and inactivation sites on the luminal side of the cardiac ryanodine receptor complex. *Circ. Res.* 87:201–206.

DelPrincipe, F., M. Egger, and E. Niggli. 1999. Calcium signalling in cardiac muscle: refractoriness revealed by coherent activation. *Nat. Cell Biol.* 1:323–329.

duBell, W. H., S. T. Gaa, W. J. Lederer, and T. B. Rogers. 1998. Independent inhibition of calcineurin and K^+ currents by the immunosuppressant FK-506 in rat ventricle. *Am. J. Physiol. Heart Circ. Physiol.* 275:H2041–H2052.

duBell, W. H., W. J. Lederer, and T. B. Rogers. 2000. K^+ currents responsible for repolarization in mouse ventricle and their modulation by FK-506 and rapamycin. *Am. J. Physiol. Heart Circ. Physiol.* 278: H886–H897.

duBell, W. H., P. A. Wright, W. J. Lederer, and T. B. Rogers. 1997. Effect of the immunosupressant FK506 on excitation–contraction coupling and outward K^+ currents in rat ventricular myocytes. *J. Physiol.* 501: 509–516.

Duke, T. A. and D. Bray. 1999. Heightened sensitivity of a lattice of membrane receptors. *Proc. Natl. Acad. Sci. U.S.A.* 96:10104–10108.

Duke, T. A., N. L. Novere, and D. Bray. 2001. Conformational spread in a ring of proteins: a stochastic approach to allostery. *J. Mol. Biol.* 308:541–553.

Fabiato, A. 1985. Calcium-induced release of calcium from the sarcoplasmic reticulum. *J. Gen. Physiol.* 85:189–320.

Fill, M., A. Zahradnikova, C. A. Villalba-Galea, I. Zahradnik, A. L. Escobar, and S. Gyorke. 2000. Ryanodine receptor adaptation. *J. Gen. Physiol.* 116:873–882.

Franzini-Armstrong, C., F. Protasi, and V. Ramesh. 1998. Comparative ultrastructure of Ca^{2+} release units in skeletal and cardiac muscle. *Ann. NY Acad. Sci.* 853:20–30.

Franzini-Armstrong, C., F. Protasi, and V. Ramesh. 1999. Shape, size, and distribution of Ca^{2+} release units and couplons in skeletal and cardiac muscles. *Biophys. J.* 77:1528–1539.

Gyorke, I., and S. Gyorke. 1998. Regulation of the cardiac ryanodine receptor channel by luminal Ca^{2+} involves luminal Ca^{2+} sensing sites. *Biophys. J.* 75:2801–2810.

Györke, S., and M. Fill. 1993. Ryanodine receptor adaptation: control mechanism of Ca^{2+}-induced Ca^{2+} release in heart. *Science.* 260: 807–809.

Haak, L. L., L. S. Song, T. F. Molinski, I. N. Pessah, H. Cheng, and J. T. Russell. 2001. Sparks and puffs in oligodendrocyte progenitors: cross talk between ryanodine receptors and inositol trisphosphate receptors. *J. Neurosci.* 21:3860–3870.

Harkins, A. B., N. Kurebayashi, and S. M. Baylor. 1993. Resting myoplasmic free calcium in frog skeletal muscle fibers estimated with fluo-3. *Biophys. J.* 65:865–881.

Hollingworth, S., C. Soeller, S. M. Baylor, and M. B. Cannell. 2000. Sarcomeric Ca^{2+} gradients during activation of frog skeletal muscle fibres imaged with confocal and two-photon microscopy. *J. Physiol.* 526:551–560.

Ikemoto, N., M. Ronjat, L. G. Mészáros, and M. Koshita. 1989. Postulated role of calsequestrin in the regulation of calcium release from sarcoplasmic reticulum. *Biochemistry.* 28:6764–6771.

Izu, L. T., J. R. Mauban, C. W. Balke, and W. G. Wier. 2001. Large currents generate cardiac Ca^{2+} sparks. *Biophys. J.* 80:88–102.

Jafri, M. S., J. J. Rice, and R. L. Winslow. 1998. Cardiac Ca^{2+} dynamics: the roles of ryanodine receptor adaptation and sarcoplasmic reticulum load. *Biophys. J.* 74:1149–1168. [Erratum. *Biophys. J.* 1998. 74:3313]

Jiang, Y. H., M. G. Klein, and M. F. Schneider. 1999. Numerical simulation of Ca^{2+} "Sparks" in skeletal muscle. *Biophys. J.* 77:2333–2357.

Keizer, J., and L. Levine. 1996. Ryanodine receptor adaptation and Ca^{2+}-induced Ca^{2+} release-dependent Ca^{2+} oscillations. *Biophys. J.* 71: 3477–3487.

Keizer, J., and G. D. Smith. 1998. Spark-to-wave transition: saltatory transmission of calcium waves in cardiac myocytes. *Biophys. Chem.* 72:87–100.

Lacampagne, A., C. W. Ward, M. G. Klein, and M. F. Schneider. 1999. Time course of individual Ca^{2+} sparks in frog skeletal muscle recorded at high time resolution. *J. Gen. Physiol.* 113:187–198.

Lederer, W. J., E. Niggli, and R. W. Hadley. 1990. Sodium–calcium exchange in excitable cells: fuzzy space. *Science.* 248:283.

Lukyanenko, V., I. Györke, and S. Györke. 1996. Regulation of calcium release by calcium inside the sarcoplasmic reticulum in ventricular myocytes. *Pflügers Arch.* 432:1047–1054.

Lukyanenko, V., S. Viatchenko-Karpinski, A. Smirnov, T. F. Wiesner, and S. Gyorke. 2001. Dynamic regulation of sarcoplasmic reticulum Ca^{2+} content and release by luminal Ca^{2+}-sensitive leak in rat ventricular myocytes. *Biophys. J.* 81:785–798.

Lukyanenko, V., T. F. Wiesner, and S. Gyorke. 1998. Termination of Ca^{2+} release during Ca^{2+} sparks in rat ventricular myocytes. *J. Physiol. (Lond)* 507:667–677.

Marks, A. R. 1996. Immunophilin modulation of calcium channel gating. *Methods.* 9:177–187.

Marx, S. O., J. Gaburjakova, M. Gaburjakova, C. Henrikson, K. Ondrias, and A. R. Marks. 2001. Coupled gating between cardiac calcium release channels (ryanodine receptors). *Circ. Res.* 88:1151–1158.

Marx, S. O., K. Ondrias, and A. R. Marks. 1998. Coupled gating between individual skeletal muscle Ca^{2+} release channels (ryanodine receptors). *Science*. 281:818–821.

Marx, S. O., S. Reiken, Y. Hisamatsu, T. Jayaraman, D. Burkhoff, N. Rosemblit, and A. R. Marks. 2000. PKA phosphorylation dissociates FKBP12.6 from the calcium release channel (ryanodine receptor): defective regulation in failing hearts. *Cell*. 101:365–376.

McCall, E., L. Li, H. Satoh, T. R. Shannon, L. A. Blatter, and D. M. Bers. 1996. Effects of FK-506 on contraction and Ca^{2+} transients in rat cardiac myocytes. *Circ. Res*. 79:1110–1121.

Meissner, G., E. Rousseau, F. A. Lai, Q. Y. Liu, and K. A. Anderson. 1988. Biochemical characterization of the Ca^{2+} release channel of skeletal and cardiac sarcoplasmic reticulum. *Mol. Cell Biochem*. 82:59–65.

Mejia-Alvarez, R., C. Kettlun, E. Rios, M. Stern, and M. Fill. 1999. Unitary Ca^{2+} current through cardiac ryanodine receptor channels under quasi-physiological ionic conditions. *J. Gen. Physiol*. 113:177–186.

Näbauer, M., and M. Morad. 1990. Ca^{2+}-induced Ca^{2+} release as examined by photolysis of caged Ca^{2+} in single ventricular myocytes. *Am. J. Physiol. Cell Physiol*. 258:C189–C193.

Negretti, N., A. Varro, and D. A. Eisner. 1995. Estimate of net calcium fluxes and sarcoplasmic reticulum calcium content during systole in rat ventricular myocytes. *J. Physiol. (Lond.)*. 486:581–591.

Niggli, E. 1999. Localized intracellular calcium signaling in muscle: calcium sparks and calcium quarks. *Annu. Rev. Physiol*. 61:311–335.

Niggli, E. and W. J. Lederer. 1990. Voltage-independent calcium release in heart muscle. *Science*. 250:565–568.

Pratusevich, V. R., and C. W. Balke. 1996. Factors shaping the confocal image of the calcium spark in cardiac muscle cells. *Biophys. J*. 71: 2942–2957.

Prestle, J., P. M. Janssen, A. P. Janssen, O. Zeitz, S. E. Lehnart, L. Bruce, G. L. Smith, and G. Hasenfuss. 2001. Overexpression of FK506-binding protein FKBP12.6 in cardiomyocytes reduces ryanodine receptor-mediated Ca^{2+} leak from the sarcoplasmic reticulum and increases contractility. *Circ. Res*. 88:188–194.

Rice, J. J., M. S. Jafri, and R. L. Winslow. 1999. Modeling gain and gradedness of Ca^{2+} release in the functional unit of the cardiac diadic space. *Biophys. J*. 77:1871–1884.

Rousseau, E., and G. Meissner. 1989. Single cardiac sarcoplasmic reticulum Ca^{2+}-release channel: activation by caffeine. *Am. J. Physiol. Heart Circ. Physiol*. 256:H328–H333.

Samso, M., and T. Wagenknecht. 1998. Contributions of electron microscopy and single-particle techniques to the determination of the ryanodine receptor three-dimensional structure. *J. Struct. Biol*. 121:172–180.

Satoh, H., L. A. Blatter, and D. M. Bers. 1997. Effects of $[Ca^{2+}]_i$, SR Ca^{2+} load, and rest on Ca^{2+} spark frequency in ventricular myocytes. *Am. J. Physiol. Heart Circ. Physiol*. 272:H657–H668.

Shacklock, P. S., W. G. Wier, and C. W. Balke. 1995. Local Ca^{2+} transients (Ca^{2+} sparks) originate at transverse tubules in rat heart cells. *J. Physiol. (Lond.)*. 487:601–608.

Sham, J. S., L. S. Song, Y. Chen, L. H. Deng, M. D. Stern, E. G. Lakatta, and H. Cheng. 1998. Termination of Ca^{2+} release by a local inactivation of ryanodine receptors in cardiac myocytes. *Proc. Natl. Acad. Sci. U.S.A*. 95:15096–15101.

Sharma, M. R., P. Penczek, R. Grassucci, H. B. Xin, S. Fleischer, and T. Wagenknecht. 1998. Cryoelectron microscopy and image analysis of the cardiac ryanodine receptor. *J. Biol. Chem*. 273:18429–18434.

Sitsapesan, R., and A. J. Williams. 2000. Do inactivation mechanisms rather than adaptation hold the key to understanding ryanodine receptor channel gating? *J. Gen. Physiol*. 116:867–872.

Smith, G. D., J. E. Keizer, M. D. Stern, W. J. Lederer, and H. Cheng. 1998. A simple numerical model of calcium spark formation and detection in cardiac myocytes. *Biophys. J*. 75:15–32.

Soeller, C., and M. B. Cannell. 1997. Numerical simulation of local calcium movements during L-type calcium channel gating in the cardiac diad. *Biophys. J*. 73:97–111.

Stern, M. D. 1992. Theory of excitation–contraction coupling in cardiac muscle. *Biophys. J*. 63:497–517.

Stern, M. D., L. S. Song, H. Cheng, J. S. Sham, H. T. Yang, K. R. Boheler, and E. Rios. 1999. Local control models of cardiac excitation–contraction coupling. A possible role for allosteric interactions between ryanodine receptors. *J. Gen. Physiol*. 113:469–489.

Tanaka, H., T. Sekine, T. Kawanishi, R. Nakamura, and K. Shigenobu. 1998. Intrasarcomere $[Ca^{2+}]$ gradients and their spatio-temporal relation to Ca^{2+} sparks in rat cardiomyocytes. *J. Physiol. (Lond.)*. 508:145–152.

Thedford, S. E., W. J. Lederer, and H. H. Valdivia. 1994. Activation of sarcoplasmic reticulum calcium release channels by intraluminal Ca^{2+}. *Biophys. J*. 66:A20.

Valdivia, H. H., J. H. Kaplan, G. C. R. Ellis-Davies, and W. J. Lederer. 1995. Rapid adaptation of cardiac ryanodine receptors: modulation by Mg^{2+} and phosphorylation. *Science*. 267:1997–2000.

Varro, A., N. Negretti, S. B. Hester, and D. A. Eisner. 1993. An estimate of the calcium content of the sarcoplasmic reticulum in rat ventricular myocytes. *Pflugers Archiv* 423:158–160.

Wagenknecht, T., M. Badermacher, R. Grassucci, J. Berkowitz, H. B. Xin, and S. Fleischer. 1997. Locations of calmodulin and FK506-binding protein on the three-dimensional architecture of the skeletal muscle ryanodine receptor. *J. Biol. Chem*. 272:32463–32471.

Wier, W. G., and C. W. Balke. 1999. Ca^{2+} release mechanisms, Ca^{2+} sparks, and local control of excitation–contraction coupling in normal heart muscle. *Circ. Res*. 85:770–776.

Xiao, R. P., H. H. Valdivia, K. Bogdanov, C. Valdivia, E. G. Lakatta, and H. P. Cheng. 1997. The immunophilin FK506-binding protein modulates Ca^{2+} release channel closure in rat heart. *J. Physiol. (Lond.)*. 500: 343–354.

Yano, M., K. Ono, T. Ohkusa, M. Suetsugu, M. Kohno, T. Hisaoka, S. Kobayashi, Y. Hisamatsu, T. Yamamoto, M. Kohno, N. Noguchi, S. Takasawa, H. Okamoto, and M. Matsuzaki. 2000. Altered stoichiometry of FKBP12.6 versus ryanodine receptor as a cause of abnormal Ca^{2+} leak through ryanodine receptor in heart failure. *Circulation*. 102: 2131–2136.

Zahradnikova, A., and I. Zahradnik. 1996. A minimal gating model for the cardiac calcium release channel. *Biophys. J*. 71:2996–3012.